

# Physiological Concentrations of Calciprotein Particles Trigger Activation and Pro-Inflammatory Response in Endothelial Cells and Monocytes

Daria Shishkova<sup>1,a</sup>, Victoria Markova<sup>1,b</sup>, Yulia Markova<sup>1,c</sup>, Maxim Sinitsky<sup>1,d</sup>,  
Anna Sinitskaya<sup>1,e</sup>, Vera Matveeva<sup>1,f</sup>, Evgenia Torgunakova<sup>1,g</sup>,  
Anastasia Lazebnaya<sup>1,h</sup>, Alexander Stepanov<sup>1,i</sup>, and Anton Kutikhin<sup>1,k\*</sup>

<sup>1</sup>Department of Experimental Medicine,  
Research Institute for Complex Issues of Cardiovascular Diseases, 650002 Kemerovo, Russia  
<sup>a</sup>e-mail: shidk@kemcardio.ru <sup>b</sup>e-mail: markve@kemcardio.ru <sup>c</sup>e-mail: markyo@kemcardio.ru  
<sup>d</sup>e-mail: sinimu@kemcardio.ru <sup>e</sup>e-mail: cepoav@kemcardio.ru <sup>f</sup>e-mail: matvvg@kemcardio.ru  
<sup>g</sup>e-mail: torgea@kemcardio.ru <sup>h</sup>e-mail: lazeai@kemcardio.ru <sup>i</sup>e-mail: stepav@kemcardio.ru  
<sup>j</sup>e-mail: kytiag@kemcardio.ru

Received November 13, 2024

Revised December 3, 2024

Accepted December 5, 2024

**Abstract**—Supraphysiological concentrations of calciprotein particles (CPPs), which are indispensable scavengers of excessive  $\text{Ca}^{2+}$  and  $\text{PO}_4^{3-}$  ions in blood, induce pro-inflammatory activation of endothelial cells (ECs) and monocytes. Here, we determined physiological levels of CPPs (10  $\mu\text{g}/\text{mL}$  calcium, corresponding to 10% increase in  $\text{Ca}^{2+}$  in the serum or medium) and investigated whether the pathological effects of calcium stress depend on the calcium delivery form, such as  $\text{Ca}^{2+}$  ions, albumin- or fetuin-centric calciprotein monomers (CPM-A/CPM-F), and albumin- or fetuin-centric CPPs (CPP-A/CPP-F). The treatment with CPP-A or CPP-F upregulated transcription of pro-inflammatory genes (*VCAM1*, *ICAM1*, *SELE*, *IL6*, *CXCL8*, *CCL2*, *CXCL1*, *MIF*) and promoted release of pro-inflammatory cytokines (IL-6, IL-8, MCP-1/CCL2, and MIP-3 $\alpha$ /CCL20) and pro- and anti-thrombotic molecules (PAI-1 and uPAR) in human arterial ECs and monocytes, although these results depended on the type of cell and calcium-containing particles. Free  $\text{Ca}^{2+}$  ions and CPM-A/CPM-F induced less consistent detrimental effects. Intravenous administration of  $\text{CaCl}_2$ , CPM-A, or CPP-A to Wistar rats increased production of chemokines (CX3CL1, MCP-1/CCL2, CXCL7, CCL11, CCL17), hepatokines (hepassocin, fetuin-A, FGF-21, GDF-15), proteases (MMP-2, MMP-3) and protease inhibitors (PAI-1) into the circulation. We concluded that molecular consequences of calcium overload are largely determined by the form of its delivery and CPPs are efficient inducers of mineral stress at physiological levels.

DOI: 10.1134/S0006297924604064

**Keywords:** calciprotein particles, calciprotein monomers, calcium ions, calcium stress, mineral stress, endothelial cells, monocytes, endothelial dysfunction, endothelial activation, systemic inflammatory response

## INTRODUCTION

Calciprotein particles (CPPs) and calciprotein monomers (CPMs) are formed through the molecular interactions between fetuin-A and nascent calcium phosphate clusters. They scavenge of excessive  $\text{Ca}^{2+}$

and  $\text{PO}_4^{3-}$  ions, thus representing an elegant mechanism for the mineral homeostasis regulation [1-6]. While albumin (by far the most abundant serum protein) is mostly responsible for the clearance of circulating  $\text{Ca}^{2+}$  ions [5, 7], fetuin-A operates as a mineral chaperone that either stabilizes calcium phosphate

**Abbreviations:** CPMs, calciprotein monomers; CPPs, concentrations of calciprotein particles; ECs, endothelial cells.

\* To whom correspondence should be addressed.

as a colloid by forming CPMs or secures its physiological aggregation into corpuscular CPPs [5, 7]. CPPs are then removed from the circulation by endothelial cells (ECs) [8-15], monocytes [13], and liver or spleen macrophages [16-19]. Generation of CPMs and CPPs is an evolutionary mechanism aimed to prevent blood supersaturation with  $\text{Ca}^{2+}$  and  $\text{PO}_4^{3-}$  ions (e.g., as a result of bone resorption) and to avert extraskeletal calcification, a pathological condition that is frequent in patients with chronic kidney disease [20-22]. Yet, internalization of CPPs by ECs and monocytes/macrophages and their digestion in lysosomes induce a chain of detrimental events including an increase in cytosolic  $\text{Ca}^{2+}$ , mitochondrial and endoplasmic reticulum stress, nuclear factor (NF)- $\kappa$ B-mediated transcriptional response, and release of pro-inflammatory cytokines, such as interleukin (IL)-6, IL-8, and monocyte chemoattractant protein 1/chemokine (C-C motif) ligand 2 (MCP-1/CCL2), ultimately contributing to the development of chronic low-grade inflammation [8-19, 23-26]. Treatment with infliximab, a selective inhibitor of tumor necrosis factor (TNF)- $\alpha$ , reduced CPM and CPP count in the serum of patients with autoimmune diseases (inflammatory bowel disease, inflammatory arthritis) [27], suggesting an efficacy of anti-inflammatory therapies in reducing CPP-related endothelial and monocyte/macrophage activation.

Currently, experimental studies employ a variety of CPP concentrations, from 25  $\mu\text{g}/\text{mL}$  [13, 15] to 100 or 200  $\mu\text{g}/\text{mL}$  calcium [16-18, 25, 28], depending on the cell type and duration of exposure. Above-median levels of ionized serum calcium ( $\text{Ca}^{2+}$ ) have been shown as a significant risk factor of cardiovascular death, as well as myocardial infarction and ischemic stroke [11, 29, 30]. The last two life-threatening conditions are driven by atherosclerosis, the development of which is triggered by endothelial activation and impaired endothelial integrity [31-35]. Average interquartile range between the risk (upper) and protective (lower) quartiles of ionized calcium is 0.12 mmol/L (i.e., 10% of the average reference value, or 4.8  $\mu\text{g}/\text{mL}$ ) [11], suggesting that in order to obtain clinically relevant results, the amount of calcium introduced to the cell culture or experimental animals should not exceed these values. Hence, an adequate quantification of CPP and CPM physiological doses should include their recalculation according to the respective mass of ionized calcium (e.g., added as  $\text{CaCl}_2$ ) in order to reach a 10% increase in the ionized calcium content in the medium.

Albeit the adverse consequences of calcium stress have been well described [36-38], it remains unclear whether its deleterious effects are determined by a calcium source (free  $\text{Ca}^{2+}$  ions, colloidal CPMs, or corpuscular CPPs) or solely depend on the amount of calcium in the microenvironment. Earlier studies have reported that stimulation of calcium-sensing

receptor by increasing the concentration of extracellular  $\text{Ca}^{2+}$  promoted internalization of CPPs, leading to the activation of NLRP3 (NLR family pyrin domain containing 3) inflammasome and IL-1 $\beta$  signaling pathway [39]. Pathological effects of CPPs largely depend on their crystallinity (amorphous primary CPPs and crystalline secondary CPPs) and density (high-density CPPs that are precipitated at  $\leq 16,000g$  and low-density CPPs that are not precipitated at this centrifugal force) [40]. The serum levels of high-density CPPs are independently and positively associated with the content of the pro-inflammatory cytokine eotaxin, whereas the levels of low-density CPPs are negatively associated with another potent inflammation inducer, IL-8 [40]. Likewise, a higher hydrodynamic radius of CPPs, which correlates with a reduced kidney function and age-dependent vascular remodeling, is associated with the cardiovascular mortality in patients with peripheral artery disease [41], as well as with vascular calcification [42] and all-cause mortality in patients with the end-stage renal disease [43]. The content of primary and secondary CPPs is associated with the vascular remodeling pathways, including those involved in collagen assembly and extracellular matrix formation [44]. CPP-induced vascular remodeling includes osteochondrogenic reprogramming of vascular smooth muscle cells, which strongly depends on the particle-size distribution, mineral composition, and crystallinity of CPPs [45]. Recent studies demonstrated an association between increased CPP counts or accelerated primary-to-secondary CPP transition with chronic kidney disease [44], ST-segment elevation myocardial infarction [46], and cardiovascular death in patients with the end-stage renal disease [47] or type 2 diabetes mellitus [48]. Removal of CPPs from blood using specific columns ameliorated chronic inflammation, endothelial dysfunction, left ventricular hypertrophy, and vascular calcification [49]. Similarly, inhibition of primary-to-secondary CPP transition prevented high phosphate-induced rat aortic calcification [50].

As indicated above, quantification of CPPs primarily relies on determining the concentration of calcium ( $\mu\text{g}$ ) per unit volume (mL) [12, 14, 16]. Artificially synthesized calcium-free magnesiprotein particles (MPPs) did not exhibit any significant toxicity after their introduction to cultured ECs cultures or animals [11], suggesting that calcium concentration is a leading factor determining the consequences of mineral stress. However, the spatiotemporal patterns of intracellular calcium distribution might differ depending on the calcium vehicle – from a steady and controlled entry of  $\text{Ca}^{2+}$  ions through the cell membrane [51, 52] to a sharp and uncurbed influx of  $\text{Ca}^{2+}$  ions into the cytosol after partial digestion of CPPs in the lysosomes [11]. These features of calcium metabolism may significantly affect transcriptional programs,

and better understanding of cellular response to circulating  $\text{Ca}^{2+}$  ions, CPMs, and CPPs is required to elucidate the pathophysiology of mineral homeostasis disorders.

Here, we investigated whether the calcium delivery form dictates the response of ECs and monocytes to physiologically relevant mineral stress that which was achieved by adding 10  $\mu\text{g}/\text{mL}$  calcium (an amount sufficient to gain a 10% increase in ionized calcium) to either cell culture medium or rat serum. We found that incubation of primary human arterial ECs with albumin-centric CPPs (CPP-A) initiated their pro-inflammatory activation manifested as an elevated production of pro-inflammatory cytokines [IL-6, IL-8, MCP-1/CCL2, macrophage inflammatory protein-3 alpha (MIP-3 $\alpha$ ), plasminogen activator inhibitor-1 (PAI-1), and urokinase-type plasminogen activator receptor (uPAR)] and verified by an increased expression of genes encoding cell adhesion molecules (VCAM1, ICAM1, E-selectin) and pro-inflammatory cytokines [IL-6, CXCL8 (chemokine (C-X-C motif) ligand 8), CCL2, and CXCL1]. Incubation with fetuin-centric CPPs (CPP-F) also promoted release of IL-6, IL-8, and MCP-1/CCL2 and upregulated expression of genes coding for cell adhesion molecules (VCAM1, ICAM1, SELE, and SELP) and pro-inflammatory cytokines (IL6, CXCL1, and MIF). Likewise, incubation of monocytes with CPP-A in the flow culture system promoted release of IL-6, IL-8, MIP-1 $\alpha$ /1 $\beta$ , MIP-3 $\alpha$ , CXCL1, CXCL5, PAI-1, uPAR, lipocalin-2, and matrix metalloproteinase-9 (MMP-9). However, addition of free  $\text{Ca}^{2+}$  ions and CPM-A caused only mild alterations in the transcriptional program and cytokine release by primary arterial ECs and monocytes. Intravenous administration of excessive  $\text{Ca}^{2+}$  ions ( $\text{CaCl}_2$ ), CPM-A, or CPP-A to Wistar rats precipitated systemic inflammatory response including an elevation in the content of multiple cytokines, hepatokines, and proteases. We suggest that the pathological effects of CPPs *in vitro* are determined by a local calcium overload, as CPPs represent calcium vehicles with a single destination (lysosomes). In contrast, the inflammatory response to the intravenous calcium bolus is less dependent on the form of calcium delivery. Nevertheless, even physiological doses of CPPs induced pro-inflammatory activation of ECs and monocytes, as well as systemic inflammatory response *in vivo*.

## MATERIALS AND METHODS

### Synthesis and quantification of CPMs and CPPs.

To prepare a mixture for the synthesis of CPMs and CPPs, 340 mg bovine serum albumin (BSA; Sigma-Aldrich, USA) or 8 mg bovine serum fetuin-A (BSF; Sigma-Aldrich) were dissolved in 4 mL of physiological saline with the subsequent addition of 2 mL of

$\text{Na}_2\text{HPO}_4$  (24 mmol/L; Sigma-Aldrich) and 2 mL of  $\text{CaCl}_2$  (40 mmol/L; Sigma-Aldrich). The mixture was resuspended after addition of each reagent. The final concentrations of reagents in the mixture were 42 mg/mL for BSA or 1 mg/mL for BSF (equal to the median serum level in a human population [11]), 10 mmol/L for  $\text{CaCl}_2$  (3.2 mg of calcium), and 6 mmol/L for  $\text{Na}_2\text{HPO}_4$ . The suspension was then aliquoted into 8 microtubes (1 mL per tube) that were placed into pre-heated (37°C) heating block (Thermit, DNA-Technology, Russia) and incubated for 10 min. After this procedure, the mixture contained three calcium sources: free  $\text{Ca}^{2+}$  ions, CPMs (either CPM-A or CPM-F), and CPPs (either CPMs-F or CPPs-F).

The resulting suspension was then aliquoted into four ultracentrifuge tubes (2 mL per tube; Beckman Coulter, USA) and centrifuged at 200,000g (OPTIMA MAX-XP, Beckman Coulter) for 1 h to sediment CPP-A/ CPP-F which were then resuspended in sterile deionized water and visualized by scanning electron microscopy (S-3400N, Hitachi, Japan) at an accelerating voltage of 10 or 30 kV after 1 : 200 dilution. To compare CPPs-A and CPPs-F with primary CPPs generated from tissue extracts or biological fluids, we employed atherosclerotic plaque-derived and serum-derived CPPs that had been generated in T-25 flasks (Wuxi NEST Biotechnology, China) for 6 weeks after adding either 3 mL of plaque extract or 3 mL of human serum, 1 mmol/L  $\text{CaCl}_2$ , and 1 mmol/L  $\text{Na}_2\text{HPO}_4$  to 7 mL of Dulbecco's Modified Eagle's Medium (DMEM; Pan-Eco, Russia) containing 10% fetal bovine serum (FBS, Capricorn Scientific, Germany), 1% L-glutamine-penicillin-streptomycin solution (Thermo Fisher Scientific, USA), and 0.4% amphotericin B (Thermo Fisher Scientific). Plaque extracts were obtained as described in [8]. After incubation for 6 weeks, CPPs were sedimented, prepared for scanning electron microscopy, and visualized as described in [8]. The supernatant with CPM-A/CPM-F and free  $\text{Ca}^{2+}$  ions was transferred into centrifugal filters with a 30-kDa molecular weight cutoff (Guangzhou Jet Bio-Filtration, China) and centrifuged at 1800g for 25 min to separate CPM-A/CPM-F (retentate) and free  $\text{Ca}^{2+}$  ions (filtrate).

The concentration of calcium in CPP-A/ CPP-F, CPM-A/CPM-F and of free  $\text{Ca}^{2+}$  ions was measured by using *o*-cresolphthalein complexone and diethanolamine-based colorimetric assay (CalciScore, AppScience Products, Russia) after 1 : 30, 1 : 10, and 1 : 10 dilution, respectively. Albumin concentration was measured using BCA Protein Assay Kit (Thermo Fisher Scientific) after 1 : 200 dilution of the CPM-containing retentate; the filtrate containing free  $\text{Ca}^{2+}$  ions was not diluted before the measurement as it was expected to be devoid of albumin. The results of colorimetric assays were detected by spectrophotometry (Multiskan Sky, Thermo Fisher Scientific) at 575 nm (calcium) and

562 nm (albumin). All procedures were performed under sterile conditions.

**Dosage estimation.** The amount calcium required for a 10% increase in the ionized calcium content in the milieu was estimated by adding 5, 10, 15, or 20  $\mu\text{g}$  of calcium (in a form of  $\text{CaCl}_2$ ) dissolved in aqueous BSA solution (300 mg/mL, average albumin concentration in the retentate) or aqueous BSF solution (28 mg/mL, average fetuin-A concentration in the retentate) per 1 mL of serum-free EndoLife cell culture medium (EL1, AppScience Products) or by adding 10, 15, 20, or 40  $\mu\text{g}$  of calcium dissolved in aqueous BSA solution (300  $\mu\text{g}/\text{mL}$ ) per 1 mL rat serum. The mixture was briefly resuspended and incubated for 1 h, after which the concentration of ionized calcium  $\text{Ca}^{2+}$ , was measured (Konelab 70i, Thermo Fisher Scientific). EndoLife medium and rat serum without  $\text{CaCl}_2$  addition were used as respective controls. According to our previous study, a 10% increase in the ionized calcium content [0.10-0.14 mmol/L (from 4.0 to 5.6  $\mu\text{g}/\text{mL}$ ); average, 0.12 mmol/L (4.8  $\mu\text{g}/\text{mL}$ ) for human serum] is equal to the interquartile range between the highest (risk) and the lowest (protective) quartiles.

**Cell culture.** Primary human coronary artery endothelial cells (HCAECs, Cell Applications, USA) and human internal thoracic artery endothelial cells (HITAECs, Cell Applications) were grown in T-75 flasks according to the manufacturer's protocol in EndoBoost Medium (EB1, AppScience Products) using 0.25% trypsin-EDTA solution (PanEco), and 10% FBS for trypsin inhibition during subculturing. Immediately before the experiments, EndoBoost Medium we replaced with serum-free EndoLife Medium, during which the cells were washed twice with warm (37°C)  $\text{Ca}^{2+}$ - and  $\text{Mg}^{2+}$ -free Dulbecco's Phosphate Buffered Saline (DPBS) (pH 7.4, BioLot) to remove the residual serum components. HCAECs and HITAECs were grown in parallel, were seeded into flow culture chambers (Ibidi, Germany) or 6-well plates (Wuxi NEST Biotechnology), and grown until reaching confluence.

Monocytes have been isolated from 5 healthy volunteers (the authors of this study) by consecutive extraction of peripheral blood mononuclear cells using a Ficoll density gradient centrifugation (Ficoll solution, 1077  $\text{g}/\text{cm}^3$ ; PanEco) and positive magnetic separation of  $\text{CD14}^+$  cells with an EasySep Magnet kit (STEMCELL Technologies, USA) and monocyte isolation kit (STEMCELL Technologies) according to the manufacturer's instructions under sterile conditions. Monocyte count was performed with an automated Countess II cell counter (Thermo Fisher Scientific) and cell counting chamber slides (Thermo Fisher Scientific).

**Internalization assay.** To analyze internalization of CPMs and CPPs by ECs, CPM-A and CPP-A were labeled with fluorescein 5-isothiocyanate-conjugated BSA (FITC-BSA, Thermo Fisher Scientific) either during

CPM/PPP synthesis (by adding 750  $\mu\text{g}$  of FITC-BSA at a 5  $\mu\text{g}/\mu\text{L}$  concentration) or after the synthesis by incubation of sedimented CPP-A with 125  $\mu\text{g}$  (25  $\mu\text{L}$ ) of FITC-BSA for 1 h at 4°C and subsequent incubation of 500  $\mu\text{L}$  of retentate (CPM-A) with 250  $\mu\text{g}$  (50  $\mu\text{L}$ ) of FITC-BSA for 1 h at 4°C after vortexing. The synthesis of CPM-A and CPP-A was performed in the dark less than 24 h before the experiment. After the labeling, sedimented CPP-A were resuspended in DPBS, centrifuged at 13,000g (Microfuge 20R, Beckman Coulter) for 10 min to wash CPP-A from unbound FITC-BSA, and resuspended in 400  $\mu\text{L}$  of DPBS.

Laminar flow was established using Ibidi Pump System Quad system (Ibidi) equipped with four separate flow culture units and Perfusion Set Yellow/Green (Ibidi). Before starting the experiment, HCAECs and HITAECs were cultured until confluence in flow culture chambers (350,000 cells per chamber) and exposed to a laminar flow (15  $\text{dyn}/\text{cm}^2$ ) using a serum-free EndoLife cell culture medium during 24 h. Next, FITC-labeled CPM-A and CPP-A were added into the system (10  $\mu\text{g}$  of calcium per 1 mL medium; 150  $\mu\text{g}$  of calcium per unit). In total, three consecutive runs were performed: (i) with CPM-A and CPP-A labeled during their synthesis; (ii) with CPM-A and CPP-A labeled after the synthesis; and (iii) with unlabeled CPM-A and CPP-A. ECs were incubated with CPM-A and CPP-A for 1 h; nuclei were counterstained with Hoechst 33342 (2  $\mu\text{g}/\text{mL}$ , Thermo Fisher Scientific) for 5 min. FITC-labeled CPM-A and CPP-A were visualized after thorough washing by confocal microscopy (LSM 700, Carl Zeiss, Germany).

To investigate colocalization of lysosomes and FITC-labeled CPMs and CPPs, CPM-A, CPM-F, CPP-A, and CPP-F were labeled with FITC after their synthesis as described above. FITC-labeled CPM-A, CPM-F, CPP-A, and CPP-F (10  $\mu\text{g}$  calcium per 1 mL medium, 4  $\mu\text{g}$  calcium per well) were added to confluent of HCAECs and HITAECs seeded into 8-well chambers (80826, Ibidi) for 3 h, and then replaced the medium with a fresh one containing the pH sensor LysoTracker Red (1  $\mu\text{mol}/\text{L}$ ; Thermo Fisher Scientific) for 1 h. Unbound FITC-BSA (60  $\mu\text{g}$ ) was used as a control; nuclei were counterstained with Hoechst 33342 for 10 min. FITC-labeled CPM-A, CPM-F, CPP-A, and CPP-F were visualized after thorough washing by confocal microscopy.

**Treatment of ECs and monocytes with free  $\text{Ca}^{2+}$  ions, CPMs, and CPPs.** To investigate the response of ECs to equal calcium concentrations delivered by different distinct vehicles, we added DPBS (control), free  $\text{Ca}^{2+}$  ions ( $\text{CaCl}_2$  as a vehicle), CPMs (either CPM-A or CPM-F), or CPPs (either CPP-A or CPP-F) (10  $\mu\text{g}$  of calcium per 1 mL cell culture medium; 20  $\mu\text{g}$  calcium per well of a 6-well plate;  $n = 18$  wells per group) to confluent HCAEC and HITAEC cultures for 24 h. We also added BSA (12 mg; i.e., average mass of albumin

in added CPM-A) or BSF (0.33 mg; i.e., average mass of fetuin-A in CPM-F) to all wells in the respective experiments for negating potential protective effects of these proteins. Serum-supplemented EndoBoost medium was replaced with serum-free EndoLife medium immediately before starting the experiment. After incubation for 24 h, the cells were examined by phase contrast microscopy; cell culture medium was removed, and the cells were washed with ice-cold (4°C) DPBS and lysed in TRIzol reagent (Thermo Fisher Scientific) to extract RNA according to the manufacturer's protocols. Cell culture medium was centrifuged at 2000g (MiniSpin Plus, Eppendorf, Germany) to remove cell debris, transferred into new tubes, and frozen at -80°C.

To evaluate the cytotoxicity of different modalities of calcium stress, we conducted colorimetric assay using water-soluble tetrazolium salt (WST)-8 and annexin V/propidium iodide staining followed by flow cytometry. For the WST-8 assay, HCAECs and HITAECS were grown in 96-well plates (Wuxi NEST Biotechnology) to confluency serum-supplemented EndoBoost medium; next, the culture medium was replaced with serum-free EndoLife medium, and added DPBS (control), free Ca<sup>2+</sup> ions (as CaCl<sub>2</sub>), CPMs (either CPM-A or CPM-F), or CPPs (either CPP-A or CPP-F) were added to the wells (10 µg calcium per 1 mL cell culture medium; 2 µg calcium per well of 96-well plate; *n* = 12 wells per group) for 24 h. Next, the medium was replaced with 100 µL of fresh serum-free EndoLife medium and 10 µL of WST-8 reagent (Wuhan Servicebio Technology, China) was added for 2 h. The products of reaction were detected spectrophotometrically at 450 nm.

For annexin V/propidium iodide staining, HCAECs and HITAECS were seeded into 6-well plates (Wuxi NEST Biotechnology) and grown to confluency in serum-supplemented EndoBoost medium. Next, the medium was replaced with serum-free EndoLife medium, and DPBS (control), free Ca<sup>2+</sup> ions (using CaCl<sub>2</sub> as a vehicle), CPMs (either CPM-A or CPM-F), or CPPs (either CPP-A or CPP-F) were added to the wells (10 µg calcium per 1 mL cell culture medium, 20 µg calcium per well of 6-well plate) for 24 h. The cells were then detached using Accutase (Capricorn Scientific) and analyzed by the annexin V/propidium iodide assay using a respective kit (ab14085, Abcam, United Kingdom) according to the manufacturer's protocol. Flow cytometry was conducted with a CytoFlex instrument using the CytExpert software (Beckman Coulter).

To study the monocyte response, we incubated monocytes (350,000 cells per unit) in serum-free EndoLife medium with equal concentrations of free Ca<sup>2+</sup> ions (CaCl<sub>2</sub>), CPM-A, or CPP-A (10 µg calcium per 1 mL culture medium; 150 µg calcium per unit; *n* = 5 donors/runs per group) in a flow culture system using

the above-mentioned perfusion set for 24 h. Similar to the previous experiment, DPBS was used as a control and BSA (87 mg, an average mass of albumin in added CPM-A) was added to all units for negating its potential protective effects. Four experimental groups (DPBS, Ca<sup>2+</sup>, CPM-A, and CPP-A) were distributed across four units of the flow culture system. The experiment was performed under sterile conditions. After 24 h of incubation, cell culture medium was collected, centrifuged at 220g (5804R, Eppendorf) to sediment monocytes and then at 2000g to remove cell debris, and then frozen at -80°C.

**Gene expression analysis.** Gene expression in Ca<sup>2+</sup>, CPM-A/CPM-F, or CPP-A/CPM-F-treated HCAECs and HITAECS was analyzed by reverse transcription-polymerase chain reaction (RT-qPCR). Briefly, cDNA was synthesized with M-MuLV-RH First Strand cDNA Synthesis Kit (R01-250, Evrogen, Russia) and reverse transcriptase M-MuLV-RH (R03-50, Evrogen), and RT-qPCR was carried out with customized primers (500 nmol/L each, Evrogen, Table S1 in the Online Resource 1), (20 ng), and BioMaster HS-qPCR Lo-ROX SYBR Master Mix (MHR031-2040, Biolabmix, Russia) according to the manufacturer's protocol. The levels of mRNAs (*VCAM1*, *ICAM1*, *SELE*, *SELP*, *IL6*, *CXCL8*, *CCL2*, *CXCL1*, *MIF*, *NOS3*, *SNAI1*, *SNAI2*, *TWIST1*, and *ZEB1* genes) were quantified by calculating  $\Delta\text{Ct}$  using the  $2^{-\Delta\text{Ct}}$  method and normalized to the average expression level of three housekeeping genes (*GAPDH*, *ACTB*, and *B2M*) and to the DPBS-treated group ( $2^{-\Delta\text{Ct}}$ ).

**Administration of free Ca<sup>2+</sup> ions, CPMs, and CPPs to Wistar rats.** The animal study protocol was approved by the Local Ethical Committee of the Research Institute for Complex Issues of Cardiovascular Diseases (protocol code, 042/2023; date of approval, April 4, 2023). Animal experiments were performed in accordance with the European Convention for the Protection of Vertebrate Animals (Strasbourg, 1986) and Directive 2010/63/EU of the European Parliament on the protection of animals used for scientific purposes. Male Wistar rats (body weight, ~300 g; estimated blood volume, ~20 mL, i.e., 6.5% of body weight) were used in the experiments. To investigate the response to the intravenous administration of various calcium sources, DPBS (control), free Ca<sup>2+</sup> ions (CaCl<sub>2</sub>), CPM-A, or CPP-A (10 µg calcium per 1 mL rat blood; 200 µg calcium per rat; *n* = 5 rats per group, *n* = 20 rats in total) were injected into the rat tail vein. BSA was added to all injections (average mass of albumin added to CPM-A, 120 mg,) for adjustment of the possible immune response to BSA. After 1 h, all rats were euthanized by intraperitoneal injection of sodium pentobarbital (100 mg/kg body weight). Serum was obtained by centrifuging rat blood at 1700g for 15 min.

**Dot blotting and enzyme-linked immunosorbent assay (ELISA).** Protein levels in the cell culture

medium were measured by dot blotting and ELISA. Dot blotting was conducted using Proteome Profiler Human XL Cytokine Array Kit (ARY022B, R&D Systems, USA) and Proteome Profiler Rat XL Cytokine Array (ARY030, R&D Systems) according to the manufacturer's instructions; proteins were visualized using chemiluminescence detection with an Odyssey XF imaging system (LI-COR Biosciences, USA). Densitometric quantification was performed using the ImageJ software (National Institutes of Health, USA). To increase dot blotting sensitivity, cell culture medium was concentrated using HyperVAC-LITE vacuum centrifugal concentrators (Gyrozen, Republic of Korea) before the measurements. Rat serum was assessed without preliminary concentrating. All culture medium samples were concentrated to the same extent: 7-fold from medium from monocytes (from 14 mL to 2 mL) and 3-fold for medium from endothelial cells (from 3 mL to 1 mL). Next, 1 mL of the concentrated medium or non-concentrated rat serum were loaded for dot blotting. The content of IL-8, IL-6, and MCP-1/CCL2 was determined by ELISA using the corresponding kits (A-8768, A-8762, and A-8782, Vector-Best, Russia) according to the manufacturer's protocols. Colorimetric detection of ELISA results was conducted spectrophotometrically at 450 nm. For ELISA measurement, 100  $\mu$ L of non-concentrated cell culture medium was used for all samples.

**Statistical analysis** was performed with GraphPad Prism 8 (GraphPad Software, USA). For RT-qPCR, the data are presented as mean  $\pm$  standard deviation (SD). Four independent groups were compared by the ordinary one-way analysis of variance (ANOVA) and subsequent Dunnett's multiple comparison test with a single pooled variance. The results of ELISA measurements are presented as median, 25th and 75th percentiles, and range. Four independent groups were compared by the Kruskal-Wallis test with subsequent Dunn's multiple comparison test. The differences were considered as statistically significant at  $p \leq 0.05$ .

## RESULTS

**Physiological relevance of CPM and CPP synthesis under conditions of mineral stress.** To investigate the effects of different calcium delivery forms on ECs and monocytes, we created a reaction mixture containing physiological concentration of BSA, physiological saline (NaCl), and supraphysiological levels of  $\text{Na}_2\text{HPO}_4$ , and  $\text{CaCl}_2$  for simultaneous generation of albumin-centric CPMs (CPM-A) and CPPs (CPP-A). Previously, similar mineral stress conditions have been used to produce fetuin-centric CPMs (CPM-F) and CPPs (CPP-F) [18]. Next, we used ultracentrifugation to isolate CPPs followed by ultrafiltration to sep-

arate CPMs (yellow retentate) from free ions and salts (transparent filtrate). Therefore, calcium was represented by (i) free  $\text{Ca}^{2+}$  ions, (ii) CPMs (colloidal form), and (iii) CPPs (corpusecular form). We used albumin to assemble CPMs (CPM-A) and CPPs (CPP-A) because a below-median content of serum albumin has been demonstrated as an independent risk factor for the coronary artery disease and ischemic stroke (in conjunction with above-median serum levels of  $\text{Ca}^{2+}$ ) [11]. Low serum albumin levels were found to correlate with a higher serum calcification propensity (i.e., CPP precipitation), while the content of albumin showed a positive correlation with total calcium (fetuin and phosphate did not display such associations) [11]. However, because fetuin-A plays a pivotal role as a mineral chaperone and governs formation of CPMs and CPPs in human blood, we also used CPM-F and CPP-F in most of the experiments. CPM-F and CPP-F were synthesized using the protocol described except that bovine serum fetuin (BSF) was used instead of BSA.

Scanning electron microscopy of CPP-A showed their sponge-like structure and irregular shape, which differed from spherical and needle-shaped appearance of primary and secondary blood-derived CPPs, respectively (Fig. 1). CPP-F had a spherical shape and sponge-like structure, thus closely resembling atherosclerotic plaque- and serum-derived primary CPPs [11]. These observations were in agreement with our previous data on the comparison of albumin-centric, fetuin-centric, plaque-derived, and serum-derived CPPs [8] and can be explained by the different cooperation of acidic serum proteins during CPP generation in the blood.

CPPs and CPMs absorbed  $\sim 30$  and  $\sim 20\%$  of calcium, respectively, whereas  $\sim 50\%$  of calcium remained in the solution as free  $\text{Ca}^{2+}$  ions. This distribution was in agreement with the physiological ratio between ionized calcium ( $\text{Ca}^{2+}$ ) and protein- and phosphate-bound calcium in human serum (1 : 1). CPPs contained from 11 to 17% of total albumin, whereas 83 to 89% of albumin remained in the retentate, thus retaining the  $\text{Ca}^{2+}$ -binding ability. The filtrate contained no BSA or BSF, which confirmed the efficiency of the ultrafiltration procedure. Taken together, these data confirmed the physiological relevance of the procedure developed for artificial synthesis of CPMs and CPPs under conditions of mineral stress.

**Physiological concentrations of CPPs cause pro-inflammatory activation of ECs and monocytes.** To determine the amount of calcium that has to be added to ensure physiological elevation in the ionized calcium content, we calculated the dose-response curve. Thus, an addition of 10  $\mu$ g of calcium per 1 mL of serum-free cell culture medium (Fig. 2a) or rat serum (Fig. 2b) was sufficient to achieve a 10% increase in the concentration of ionized calcium (i.e., the interquartile range between the risk and protective

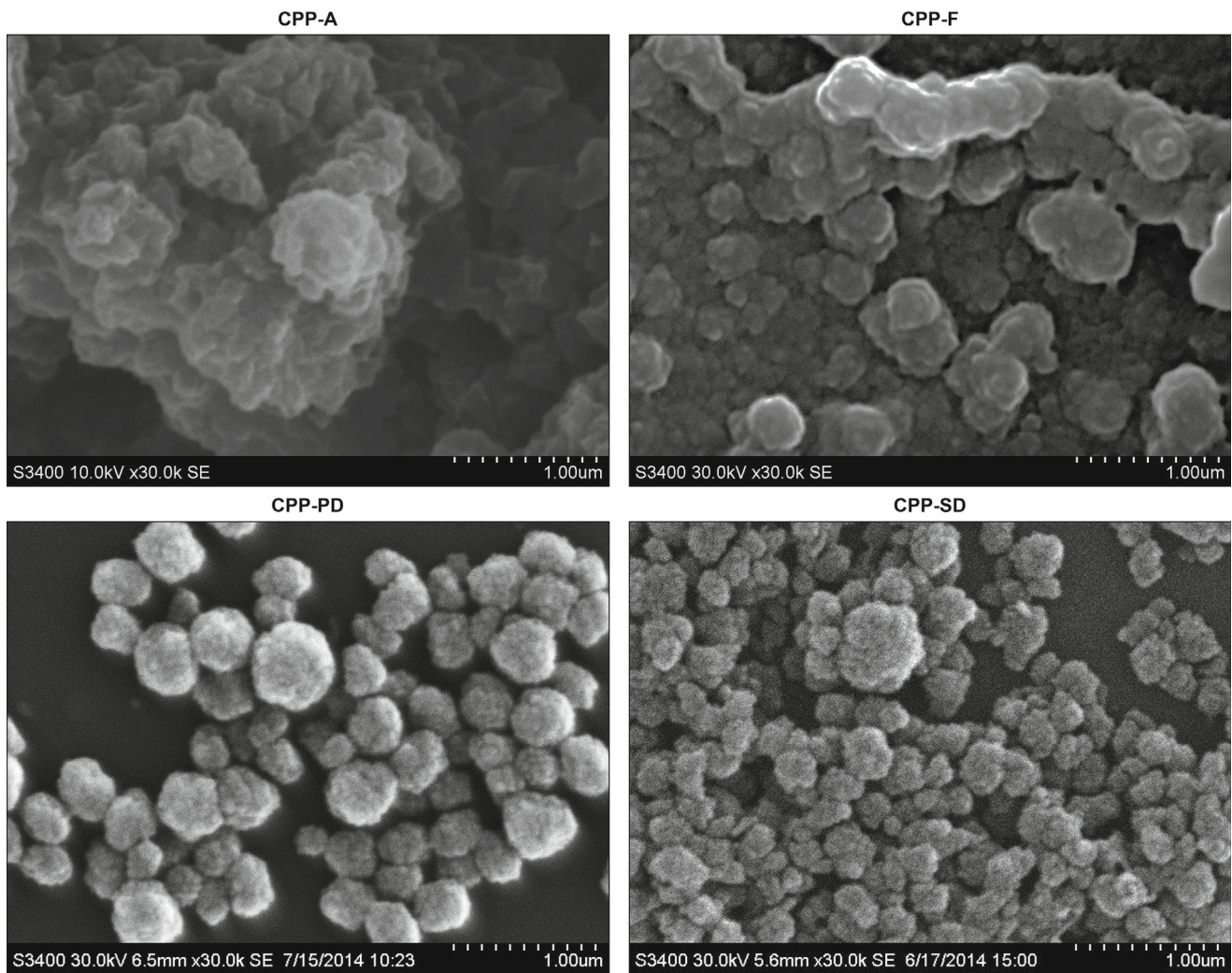


**Fig. 1.** Scanning electron microscopy images of albumin-centric (CPP-A), fetuin-centric (CPP-F), calcified atherosclerotic plaque-derived (CPP-PD), and serum-derived (CPP-SD) CPPs. Secondary electron mode; acceleration voltage, 10 kV (CPP-A) or 30 kV (CPP-F, CPP-PD, and CPP-SD); magnification,  $\times 30,000$ ; scale bar: 1  $\mu\text{m}$ .

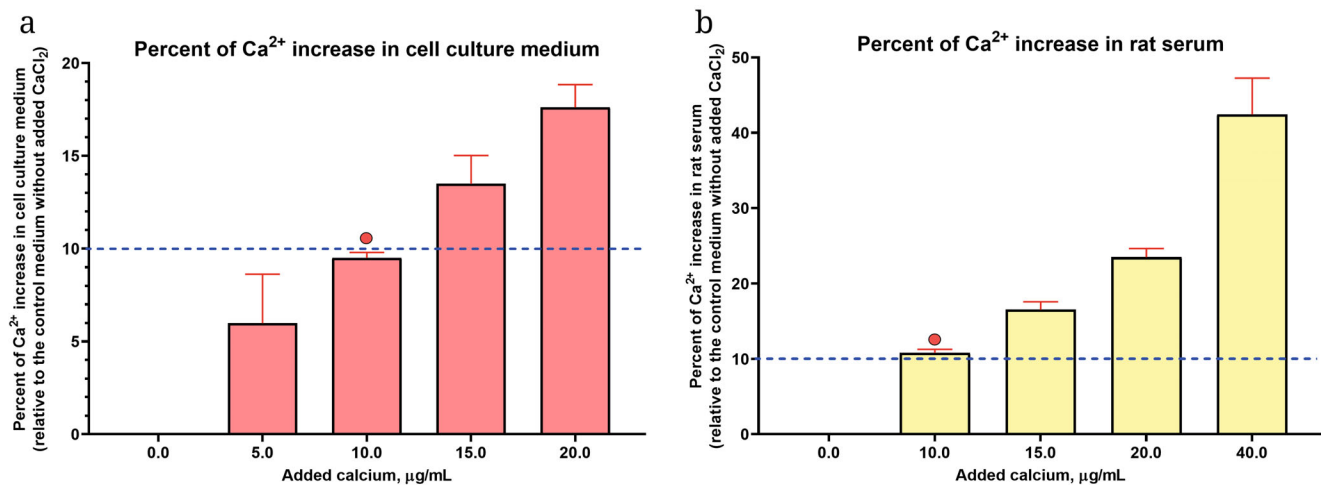


**Fig. 2.** Increase in the ionized calcium ( $\text{Ca}^{2+}$ ) concentration in (a) cell culture medium and (b) rat serum upon addition of increasing amounts of  $\text{CaCl}_2$ ; x-axis, concentration of added calcium; y-axis, increase in  $\text{Ca}^{2+}$  concentration relative to the control medium or serum without calcium addition. An increase in the  $\text{Ca}^{2+}$  concentration by 10% (blue dashed line) was achieved by the addition of 10  $\mu\text{g}$  of calcium per 1 mL of cell culture medium or rat serum (red circle).

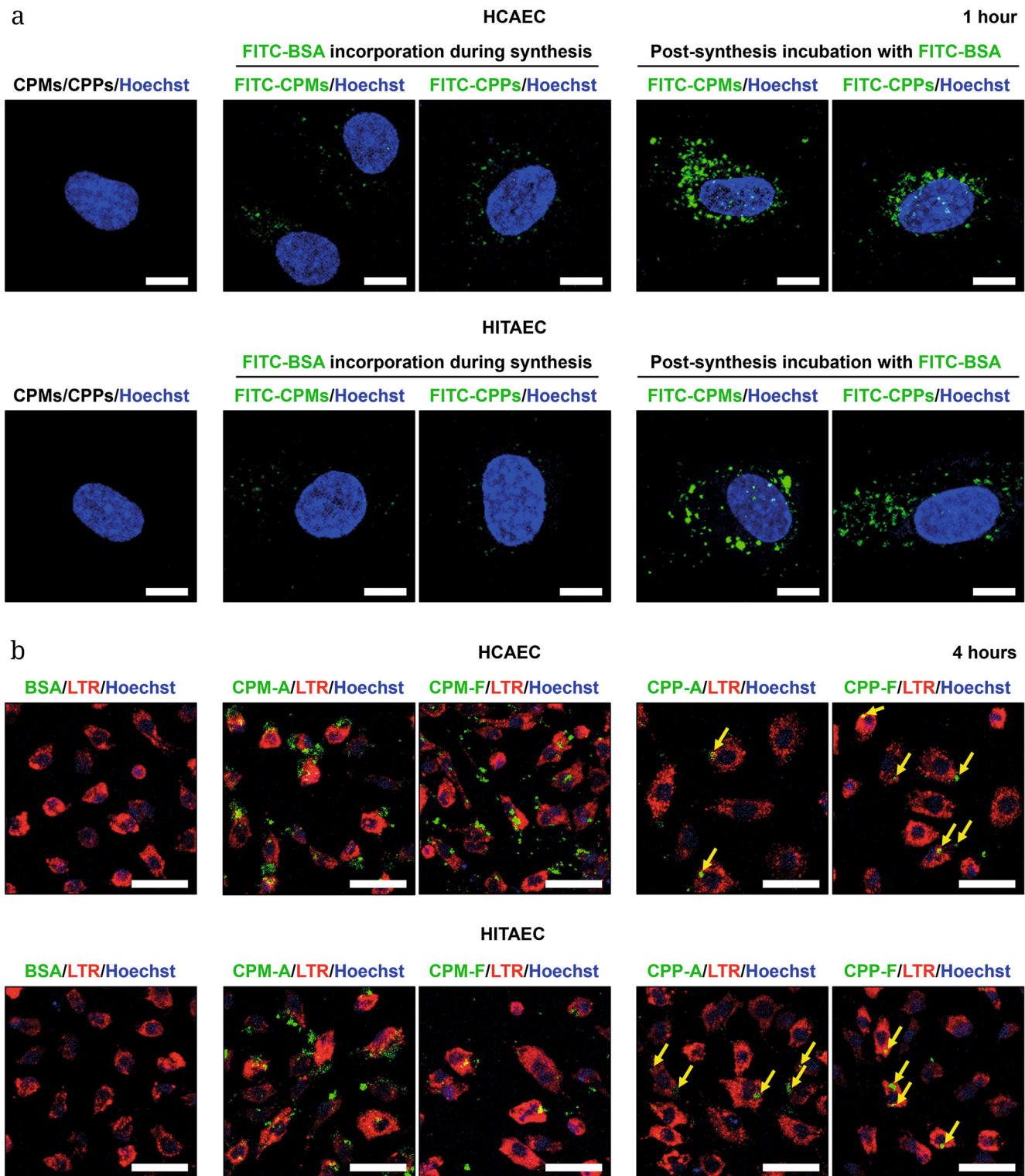


**Fig. 3.** Internalization of FITC-BSA-labeled CPMs (FITC-CPMs) and CPPs (FITC-CPPs) by HCAECs and HITAECs. **a)** Comparison of signal intensities of internalized FITC-CPMs and FITC-CPPs obtained by two different labeling techniques. ECs were treated for 1 h with unlabeled CPMs and CPPs (left panel), CPMs and CPPs that incorporated FITC-BSA during their synthesis (central panel), and CPMs and CPPs that were incubated with FITC-BSA after their synthesis (right panel). Nuclei were counterstained with Hoechst 33342. Confocal microscopy; magnification,  $\times 630$ ; scale bar, 5  $\mu\text{m}$ . **b)** Lysosomes stained with LysoTracker Red (LTR) in ECs treated for 4 h with CPMs (FITC-CPM-A and FITC-CPM-F) or CPPs (FITC-CPP-A and FITC-CPP-F): left panel, free FITC-BSA; central panel: CPM-A and CPM-F co-incubated with FITC-BSA during their synthesis; right panel, CPP-A and CPP-F co-incubated with FITC-BSA after their synthesis. Yellow arrows indicate CPP-A and CPP-F inside the cells. Nuclei were counterstained with Hoechst 33342. Confocal microscopy; magnification,  $\times 200$ ; scale bar, 50  $\mu\text{m}$ .

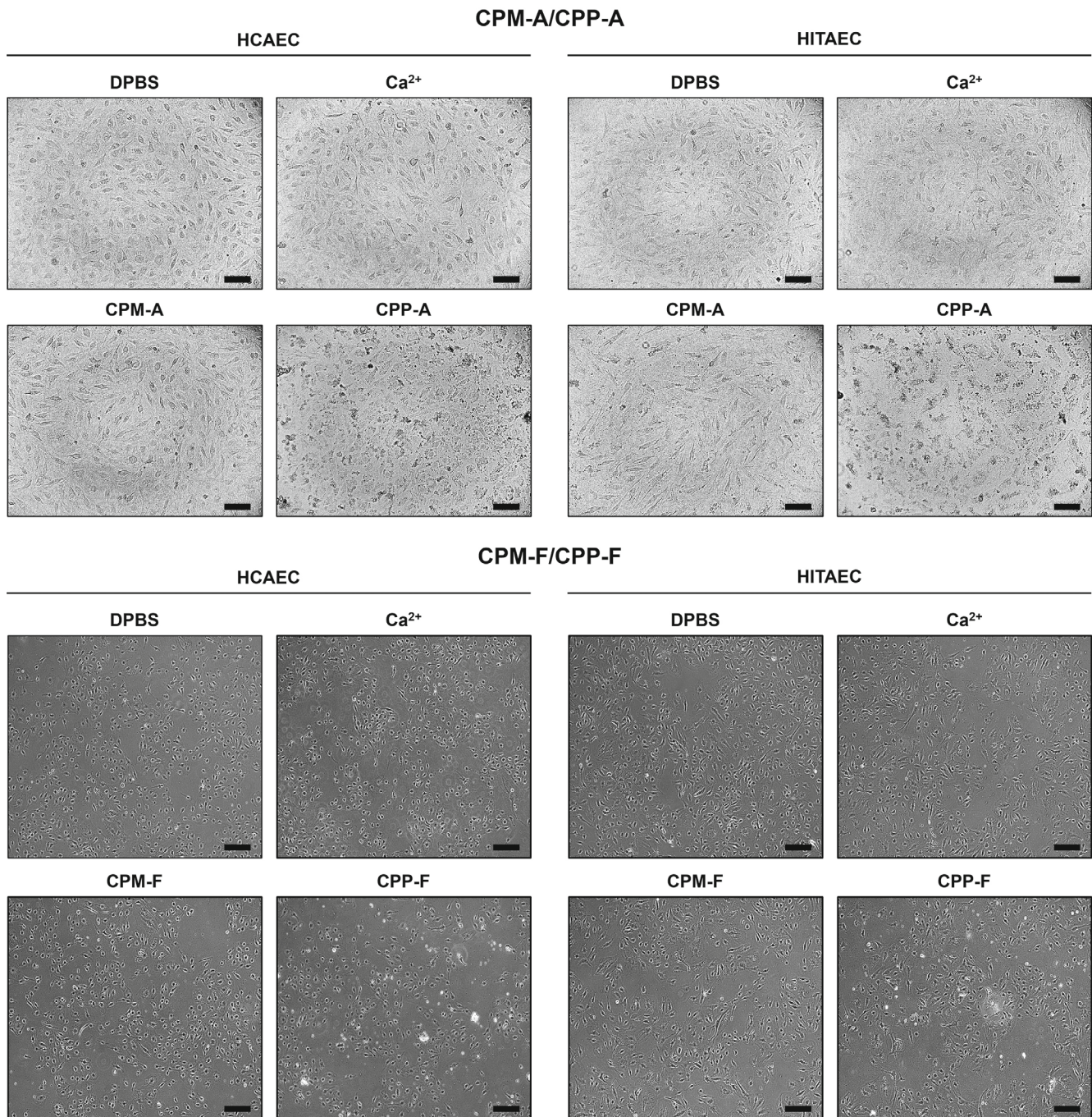


**Fig. 4.** Bright-field microscopy (CPM-A/ CPP-A, top) and phase-contrast microscopy (CPM-F/ CPP-F, bottom) of HCAECs (left panels) and HITAECS (right panels) treated with DPBS (control), free Ca<sup>2+</sup> ions, CPMs (CPM-A, top; CPM-F, bottom), or CPPs (CPP-A, top; CPP-F, bottom) (10 µg of calcium per 1 mL serum-free cell culture medium) for 24 h; magnification, ×200; scale bar, 100 µm.

quartiles in the population). Hence, we selected 10 µg/mL as the optimal calcium concentration to model clinically relevant mineral stress. Further experiments included four groups: 1) control (DPBS); 2) free Ca<sup>2+</sup> ions delivered as CaCl<sub>2</sub>; 3) either CPM-A or CPM-F; 4) either CPP-A or CPP-F.

We then asked whether CPMs are internalized in a flow system in a similar manner as CPPs. To address

this question, we labeled CPM-A and CPP-A with FITC-BSA either during CPM-A/ CPP-A generation (by adding FITC-BSA to the solution) or after their formation by incubation of sedimented CPP-A and separated CPM-A with FITC-BSA. An intense green fluorescence was evident in ECs already 1 h after addition of FITC-labeled CPM-A and CPP-A to the flow culture system (Fig. 3a). CPM-A and CPP-A incubated with FITC-BSA after their

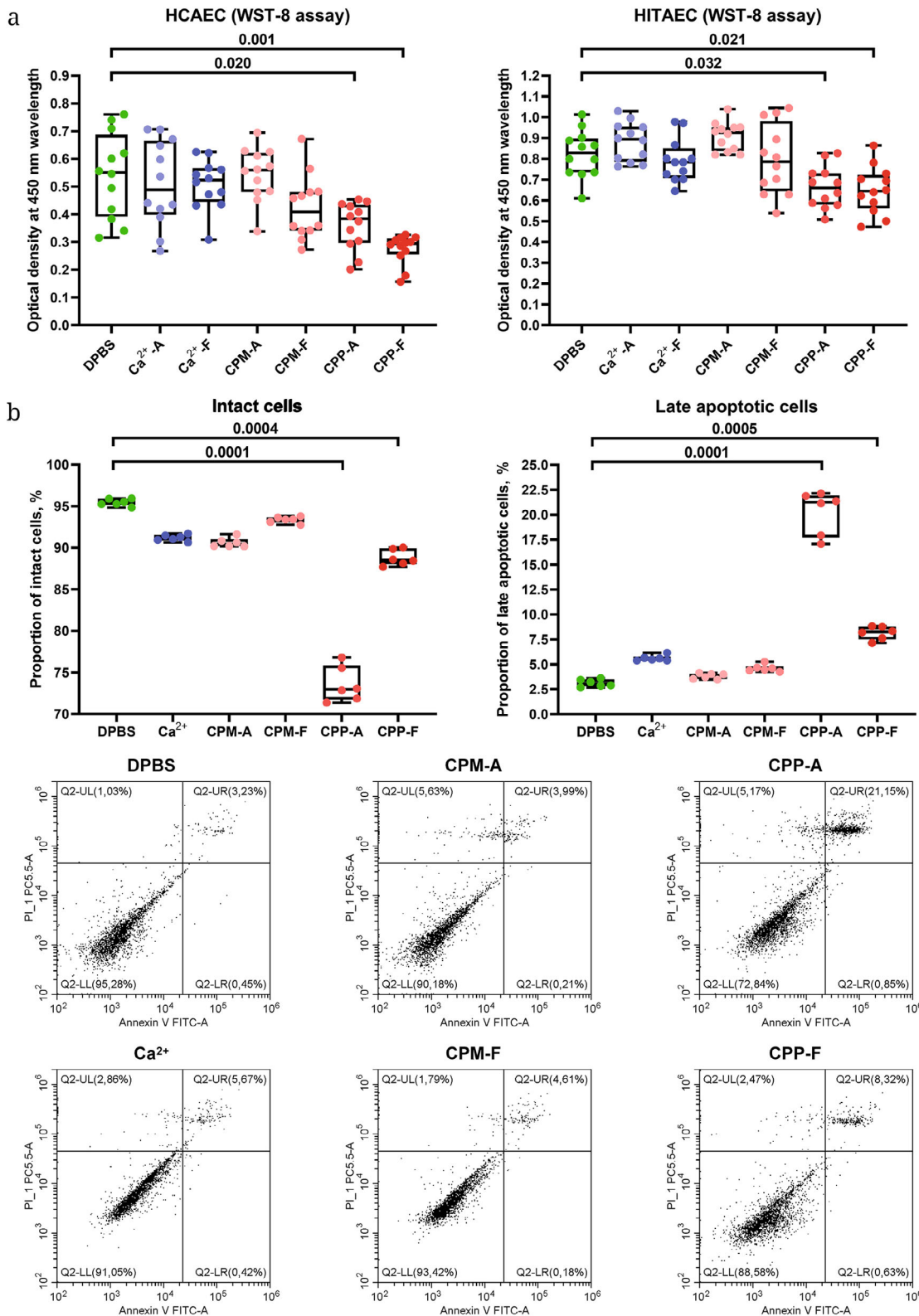


**Fig. 5.** Cytotoxicity assay after incubation of HCAECs (left panel) and HITAEC (right panel) with DPBS (control), free Ca<sup>2+</sup> ions, CPMs (CPM-A or CPM-F), or CPPs (CPP-A or CPP-F) (10 µg of calcium per 1 mL serum-free cell culture medium) for 24 h: a) WST-8 colorimetric assay (evaluation of WST-8 reduction by intracellular dehydrogenases to a water-soluble orange-yellow formazan compound with the maximum absorption at 450 nm). b) Annexin V and propidium iodide assay (lower left quadrant Q2-LL, normal cells; lower right quadrant Q2-LR, early apoptotic cells; upper right quadrant Q2-UR, late apoptotic cells; upper left quadrant Q2-UL, necrotic cells). Top panel, statistical analysis of the content of intact and late apoptotic cells. Bottom panel: representative flow cytometry plots.

synthesis produced a significantly higher fluorescence signal comparison to those that incorporated FITC-BSA during their synthesis (Fig. 3a). Similar fluorescence intensity for CPM-A and CPP-A suggested that FITC-BSA had the same affinity for both these species (Fig. 3a). Identification of FITC-labeled CPMs/CPs in lysosomes stained with the pH sensor LysoTracker Red confirmed internalization of CPM-A, CPM-F, CPP-A, and CPP-F by HCAECs and HITAECs after 4 h of incubation, while FITC-BSA itself did not enter ECs (Fig. 3b).

To compare the pathological effects of different calcium delivery forms on ECs, we added  $\text{Ca}^{2+}$ , CPM-A/CPM-F, or CPP-A/CP-P (10  $\mu\text{g}/\text{mL}$ ) to HCAECs and HITAECs. Using bright-field and phase contrast microscopies, we observed pathological alterations (i.e., loss of intercellular contacts, cell shrinkage and detachment) in ECs after incubation with CPP-A or CPP-F, but not with  $\text{Ca}^{2+}$  or CPM-A/CPM-F (Fig. 4).

To further investigate the cytotoxicity of CPP-A and CPP-F, we assessed a decrease in the cell viability and metabolism in different modes of calcium stress using WST-8 colorimetric assay. After 24-hour incubation with CPP-A or CPP-F, the intensity of cell metabolism dropped in both HCAECs and HITAECs (Fig. 5a). Flow cytometry analysis of cell death using annexin V and propidium iodide staining identified that a significant proportion of ECs underwent apoptosis after 24 h of treatment with CPP-A or CPP-F (Fig. 5b).

RT-qPCR demonstrated a significant increase in the expression of genes encoding cell adhesion molecules (*VCAM1*, *ICAM1*, and *SELE*) and pro-inflammatory cytokines (*IL6*, *CXCL8*, *CCL2*, and *CXCL1*) in HCAECs treated with CPP-A (Table 1). Exposure to CPP-F triggered a similar response, which included elevated expression of *VCAM1*, *SELP*, *IL6*, and *MIF* genes along with a trend towards a significant increase in the expression of *ICAM1* and *SELE* genes (Table 2).

**Table 1.** Relative gene expression ( $\Delta\text{Ct}$ ; fold change;  $p$ -value) in HCAECs and HITAECs treated with DPBS (control), free  $\text{Ca}^{2+}$  ions, CPM-A, or CPP-A (10  $\mu\text{g}$  of calcium per 1 mL of serum-free cell culture medium) for 24 h

Gene	Metrics	HCAEC				HITAEC			
		DPBS	$\text{Ca}^{2+}$	CPM-A	CPP-A	DPBS	$\text{Ca}^{2+}$	CPM-A	CPP-A
<i>VCAM1</i>	$\Delta\text{Ct}$	0.0003 $\pm$ 0.0006	0.0001 $\pm$ 0.0001	0.0002 $\pm$ 0.0001	0.0015 $\pm$ 0.0010	0.0003 $\pm$ 0.0002	0.0011 $\pm$ 0.0011	0.0006 $\pm$ 0.0004	0.0010 $\pm$ 0.0008
	fold change	1	0.52	0.76	<b>6.00</b>	1	<b>3.67</b>	2.00	<b>3.33</b>
	$p$ -value	1.00	0.904	0.985	<b>0.001</b>	1.00	<b>0.009</b>	0.463	<b>0.029</b>
<i>ICAM1</i>	$\Delta\text{Ct}$	0.0148 $\pm$ 0.0066	0.0372 $\pm$ 0.0210	0.0118 $\pm$ 0.0034	0.1169 $\pm$ 0.0837	0.0338 $\pm$ 0.0213	0.0503 $\pm$ 0.0339	0.0404 $\pm$ 0.0244	0.0432 $\pm$ 0.0201
	fold change	1	2.52	0.80	<b>7.90</b>	1	1.49	1.20	1.28
	$p$ -value	1.00	0.320	0.994	<b>0.001</b>	1.00	0.148	0.782	0.559
<i>SELE</i>	$\Delta\text{Ct}$	0.0056 $\pm$ 0.0026	0.0089 $\pm$ 0.0036	0.0020 $\pm$ 0.0009	0.0134 $\pm$ 0.0065	0.0595 $\pm$ 0.0351	0.1049 $\pm$ 0.1387	0.0909 $\pm$ 0.1203	0.0943 $\pm$ 0.0872
	fold change	1	<b>1.59</b>	<b>0.36</b>	<b>2.39</b>	1	1.76	1.53	1.58
	$p$ -value	1.00	<b>0.041</b>	<b>0.026</b>	<b>0.001</b>	1.00	0.415	0.687	0.619
<i>SELP</i>	$\Delta\text{Ct}$	0.0077 $\pm$ 0.0067	0.0027 $\pm$ 0.0008	0.0015 $\pm$ 0.0009	0.0026 $\pm$ 0.0023	0.0009 $\pm$ 0.0006	0.0054 $\pm$ 0.0058	0.0056 $\pm$ 0.0055	0.0025 $\pm$ 0.0030
	fold change	1	<b>0.35</b>	<b>0.19</b>	<b>0.34</b>	1	<b>6.00</b>	<b>6.22</b>	2.78
	$p$ -value	1.00	<b>0.001</b>	<b>0.001</b>	<b>0.001</b>	1.00	<b>0.008</b>	<b>0.005</b>	0.567

Table 1 (cont.)

Gene	Metrics	HCAEC				HITAEC			
		DPBS	Ca <sup>2+</sup>	CPM-A	CPP-A	DPBS	Ca <sup>2+</sup>	CPM-A	CPP-A
<i>IL6</i>	$\Delta$ Ct	0.0182 ± 0.0131	0.0058 ± 0.0023	0.0072 ± 0.0045	0.1197 ± 0.0837	0.0085 ± 0.0043	0.0132 ± 0.0155	0.0197 ± 0.0214	0.0247 ± 0.0272
	fold change	1	0.32	0.40	<b>6.58</b>	1	1.55	2.32	<b>2.91</b>
	<i>p</i> -value	1.00	0.729	0.796	<b>0.001</b>	1.00	0.803	0.196	<b>0.035</b>
<i>CXCL8</i>	$\Delta$ Ct	0.0371 ± 0.0260	0.0441 ± 0.0152	0.0250 ± 0.0105	2.1412 ± 1.5287	0.1396 ± 0.0561	0.1801 ± 0.2005	0.1825 ± 0.1871	0.3279 ± 0.3681
	fold change	1	1.19	0.67	<b>57.71</b>	1	1.29	1.31	<b>2.35</b>
	<i>p</i> -value	1.00	0.999	0.999	<b>0.001</b>	1.00	0.914	0.901	<b>0.045</b>
<i>CCL2</i>	$\Delta$ Ct	0.7514 ± 0.6502	0.4398 ± 0.4293	0.6965 ± 0.6669	1.3616 ± 1.0636	0.8908 ± 0.4072	1.2866 ± 1.5286	1.4987 ± 1.6929	1.6162 ± 1.9876
	Fold change	1	0.59	0.93	<b>1.81</b>	1	1.44	1.68	1.81
	<i>p</i> -value	1.00	0.448	0.992	<b>0.042</b>	1.00	0.777	0.494	0.353
<i>CXCL1</i>	$\Delta$ Ct	0.1267 ± 0.0562	0.0436 ± 0.0408	0.0444 ± 0.0343	0.3486 ± 0.1551	0.0647 ± 0.0279	0.1520 ± 0.1842	0.0944 ± 0.0885	0.0983 ± 0.1052
	fold change	1	<b>0.34</b>	<b>0.35</b>	<b>2.75</b>	1	2.35	1.46	1.52
	<i>p</i> -value	1.00	<b>0.017</b>	<b>0.018</b>	<b>0.001</b>	1.00	0.069	0.782	0.715
<i>MIF</i>	$\Delta$ Ct	0.3853 ± 0.1660	0.2309 ± 0.1040	0.2731 ± 0.0839	0.4170 ± 0.2857	0.2753 ± 0.1576	0.7919 ± 0.9280	0.5270 ± 0.4019	0.4618 ± 0.4146
	fold change	1	<b>0.60</b>	0.71	1.08	1	<b>2.88</b>	1.91	1.68
	<i>p</i> -value	1.00	<b>0.031</b>	0.155	0.910	1.00	<b>0.018</b>	0.386	0.618
<i>NOS3</i>	$\Delta$ Ct	0.0094 ± 0.0063	0.0069 ± 0.0036	0.0069 ± 0.0033	0.0091 ± 0.0087	0.0031 ± 0.0018	0.0093 ± 0.0090	0.0119 ± 0.0126	0.0060 ± 0.0037
	fold change	1	0.73	0.73	0.97	1	<b>3.00</b>	<b>3.84</b>	1.94
	<i>p</i> -value	1.00	0.473	0.475	0.997	1.00	<b>0.050</b>	<b>0.005</b>	0.547
<i>SNAI1</i>	$\Delta$ Ct	0.0168 ± 0.0101	0.0100 ± 0.0040	0.0124 ± 0.0065	0.0344 ± 0.0291	0.0049 ± 0.0020	0.0129 ± 0.0110	0.0140 ± 0.0124	0.0094 ± 0.0100
	fold change	1	0.60	0.74	<b>2.05</b>	1	<b>2.63</b>	<b>2.86</b>	1.92
	<i>p</i> -value	1.00	0.487	0.771	<b>0.009</b>	1.00	<b>0.042</b>	<b>0.018</b>	0.371

Table 1 (cont.)

Gene	Metrics	HCAEC				HITAEC			
		DPBS	Ca <sup>2+</sup>	CPM-A	CPP-A	DPBS	Ca <sup>2+</sup>	CPM-A	CPP-A
<i>SNAI2</i>	ΔCt	0.0129 ± 0.0103	0.0038 ± 0.0009	0.0065 ± 0.0046	0.0047 ± 0.0032	0.0009 ± 0.0007	0.0033 ± 0.0022	0.0099 ± 0.0160	0.0030 ± 0.0055
	fold change	1	<b>0.29</b>	<b>0.50</b>	<b>0.36</b>	1	3.67	<b>11.00</b>	3.33
	<i>p</i> -value	1.00	<b>0.001</b>	<b>0.005</b>	<b>0.001</b>	1.00	0.784	<b>0.015</b>	0.841
<i>TWIST1</i>	ΔCt	0.0015 ± 0.0012	0.0003 ± 0.0002	0.0002 ± 0.0001	0.0009 ± 0.0008	0.0004 ± 0.0004	0.0018 ± 0.0026	0.0037 ± 0.0077	0.0016 ± 0.0016
	fold change	1	<b>0.20</b>	<b>0.13</b>	0.60	1	4.50	9.25	4.00
	<i>p</i> -value	1.00	<b>0.001</b>	<b>0.001</b>	0.150	1.00	0.742	0.170	0.874
<i>ZEB1</i>	ΔCt	0.2376 ± 0.1200	0.0779 ± 0.0561	0.1607 ± 0.0596	0.3277 ± 0.2237	0.1438 ± 0.0686	0.3697 ± 0.4382	0.4552 ± 0.4601	0.3559 ± 0.4082
	fold change	1	<b>0.33</b>	0.68	1.38	1	2.57	<b>3.17</b>	2.47
	<i>p</i> -value	1.00	<b>0.002</b>	0.209	0.117	1.00	0.201	<b>0.049</b>	0.244

Note. Genes encoding pro-inflammatory cell adhesion molecules (*VCAM1*, *ICAM1*, *SELE*, *SELP*), pro-inflammatory cytokines (*IL6*, *CXCL8*, *CCL2*, *CXCL1*, *MIF*), endothelial nitric oxide synthase (*NOS3*), and endothelial-to-mesenchymal transition transcription factors (*SNAI1*, *SNAI2*, *TWIST1*, *ZEB1*) were analyzed. Significant fold change values and *p*-values are shown in bold; ΔCt is shown as mean ± SD.

The same gene expression pattern was observed for HITAECs, including CPP-A-induced activation of expression of *VCAM1*, *IL6*, and *CXCL8* genes (Table 1), while incubation with CPP-F upregulated expression of *SELE*, *SELP*, *CXCL1*, and *MIF* genes (Table 2). Collectively, these molecular signatures pointed towards the development of pro-inflammatory endothelial activation and suggested elevation in the content of pro-inflammatory cytokines in cell culture medium. In contrast to CPP-A/PP-F, free Ca<sup>2+</sup> ions and CPM-A/CPM-F induced a stochastic rather than a consistent response which did not reflect endothelial dysfunction.

Treatment with CPP-A significantly increased expression of inducible endothelial pro-inflammatory cytokines (IL-6, IL-8, and MCP-1/CCL2) in the cell culture medium for both HCAECs and HITAECs (Fig. 6), while addition of free Ca<sup>2+</sup> ions and CPM-A caused no stable pathological response at the protein level, thus corroborating the results of gene expression profiling (Fig. 6). Incubation with CPP-F also promoted expression of above-mentioned cytokines in HCAECs and HITAECs, whereas free Ca<sup>2+</sup> ions and CPM-F caused a cytokine response in HITAECs (Fig. 7).

To further explore the release of cytokines upon calcium overload, we performed a semi-quantitative dot blotting analysis of serum-free cell culture medium from HCAECs and HITAECs treated with Ca<sup>2+</sup>, CPM-A, and CPP-A. CPP-A increased production of PAI-1 (also called serpin E1), chemokine (C-X-C motif) ligand 1 (CXCL1), MCP-1/CCL2, IL-8, macrophage migration inhibitory factor (MIF), and soluble CD105 and CD147 proteins has been elevated in HCAECs, as well as upregulated the synthesis of ST2 (suppression of tumorigenicity 2) and RANTES/CCL5 [regulated on activation, normal T cell expressed and secreted/chemokine (C-C motif) ligand 5] in HITAECs (Fig. 8 and Table S1 in the Online Resource 1). The levels of soluble uPAR and MIP-3α/CCL20 were elevated in the cell culture supernatant in both EC lines after incubation with CPP-A (Fig. 8 and Table 1), i.e., exposure to CPP-A induced the release of 11 cytokines (Fig. 8 and Table S1 in the Online Resource 1). Six of these pro-inflammatory molecules (CXCL1, MCP-1/CCL2, MIF, uPAR, sCD147, and ST2 protein) were also overrepresented in the cell culture supernatant collected from CPM-A-treated ECs, while five proteins [CXCL1, sCD147, ST2 protein, platelet-derived growth factor AA (PDGF-AA),

**Table 2.** Relative gene expression ( $\Delta$ Ct, fold change, and  $p$ -value) in HCAECs and HITAECs treated with control DPBS, free  $\text{Ca}^{2+}$  ions, CPM-F, and CPP-F (5  $\mu\text{g}$  of calcium per 1 mL of serum-free cell culture medium) for 24 h

Gene	Metrics	HCAEC				HITAEC			
		DPBS	$\text{Ca}^{2+}$	CPM-F	CPP-F	DPBS	$\text{Ca}^{2+}$	CPM-F	CPP-F
<i>VCAM1</i>	$\Delta$ Ct	0.0020 $\pm$ 0.0015	0.0019 $\pm$ 0.0007	0.0018 $\pm$ 0.0009	0.0042 $\pm$ 0.0032	0.0004 $\pm$ 0.0003	0.0004 $\pm$ 0.0002	0.0005 $\pm$ 0.0003	0.0006 $\pm$ 0.0005
	fold change	1	0.95	0.90	<b>2.1</b>	1	0.95	1.28	1.54
	$p$ -value	1.00	0.998	0.984	<b>0.008</b>	1.00	0.995	0.628	0.113
<i>ICAM1</i>	$\Delta$ Ct	0.0540 $\pm$ 0.0510	0.0165 $\pm$ 0.0133	0.0208 $\pm$ 0.0266	0.1011 $\pm$ 0.1201	0.0646 $\pm$ 0.0282	0.0906 $\pm$ 0.0503	0.0820 $\pm$ 0.0306	0.0885 $\pm$ 0.0519
	fold change	1	0.31	0.39	1.87	1	1.40	1.27	1.37
	$p$ -value	1.00	0.229	0.319	0.098	1.00	0.159	0.454	0.213
<i>SELE</i>	$\Delta$ Ct	0.0048 $\pm$ 0.0037	0.0082 $\pm$ 0.0107	0.0028 $\pm$ 0.0019	0.0091 $\pm$ 0.0053	0.0018 $\pm$ 0.0007	0.0084 $\pm$ 0.0055	0.0069 $\pm$ 0.0032	0.0058 $\pm$ 0.0061
	fold change	1	1.71	0.58	1.90	1	<b>4.67</b>	<b>3.83</b>	<b>3.22</b>
	$p$ -value	1.00	0.441	0.879	0.375	1.00	<b>0.001</b>	<b>0.003</b>	<b>0.023</b>
<i>SELP</i>	$\Delta$ Ct	0.0119 $\pm$ 0.0131	0.0060 $\pm$ 0.0060	0.0089 $\pm$ 0.0079	0.0318 $\pm$ 0.0276	0.0050 $\pm$ 0.0023	0.0032 $\pm$ 0.0016	0.0035 $\pm$ 0.0017	0.0078 $\pm$ 0.0053
	fold change	1	0.50	0.75	<b>2.67</b>	1	0.64	0.70	<b>1.56</b>
	$p$ -value	1.00	0.534	0.895	<b>0.002</b>	1.00	0.227	0.374	<b>0.025</b>
<i>IL6</i>	$\Delta$ Ct	0.0072 $\pm$ 0.0029	0.0100 $\pm$ 0.0097	0.0063 $\pm$ 0.0046	0.0233 $\pm$ 0.0188	0.0044 $\pm$ 0.0016	0.0045 $\pm$ 0.0045	0.0031 $\pm$ 0.0012	0.0064 $\pm$ 0.0042
	fold change	1	1.39	0.88	<b>3.24</b>	1	1.02	0.70	1.45
	$p$ -value	1.00	0.783	0.988	<b>0.001</b>	1.00	0.999	0.463	0.191
<i>CXCL8</i>	$\Delta$ Ct	0.1330 $\pm$ 0.0572	0.2582 $\pm$ 0.1501	0.1892 $\pm$ 0.0573	0.1632 $\pm$ 0.0898	0.0294 $\pm$ 0.0175	0.0636 $\pm$ 0.0714	0.0366 $\pm$ 0.0185	0.0522 $\pm$ 0.0411
	fold change	1	<b>1.94</b>	1.42	1.23	1	2.16	1.24	1.78
	$p$ -value	1.00	<b>0.001</b>	0.203	0.668	1.00	0.053	0.924	0.272
<i>CCL2</i>	$\Delta$ Ct	1.1073 $\pm$ 0.3168	2.8331 $\pm$ 1.9144	1.1255 $\pm$ 0.3747	1.3772 $\pm$ 0.8673	0.3096 $\pm$ 0.0759	0.5079 $\pm$ 0.3852	0.4625 $\pm$ 0.1941	0.5145 $\pm$ 0.3698
	Fold change	1	<b>2.56</b>	1.02	1.24	1	1.64	1.49	1.66
	$p$ -value	1.00	<b>0.001</b>	0.999	0.795	1.00	0.105	0.265	0.090

Table 2 (cont.)

Gene	Metrics	HCAEC				HITAEC			
		DPBS	Ca <sup>2+</sup>	CPM-F	CPP-F	DPBS	Ca <sup>2+</sup>	CPM-F	CPP-F
<i>CXCL1</i>	$\Delta$ Ct	0.3756 ± 0.1000	0.6205 ± 0.3781	0.4173 ± 0.1658	0.5612 ± 0.3499	0.0543 ± 0.0156	0.1053 ± 0.0885	0.0831 ± 0.0437	0.1477 ± 0.1538
	fold change	1	<b>1.65</b>	1.11	1.49	1	1.94	1.53	<b>2.72</b>
	<i>p</i> -value	1.00	<b>0.026</b>	0.942	0.117	1.00	0.235	0.668	<b>0.009</b>
<i>MIF</i>	$\Delta$ Ct	2.8076 ± 0.9811	2.6168 ± 1.6847	2.2889 ± 0.8340	5.5963 ± 3.2599	0.2999 ± 0.0856	0.4214 ± 0.3609	0.3627 ± 0.1458	0.6572 ± 0.5581
	fold change	1	0.93	0.82	<b>1.99</b>	1	1.41	1.21	<b>2.19</b>
	<i>p</i> -value	1.00	0.983	0.763	<b>0.001</b>	1.00	0.583	0.904	<b>0.007</b>
<i>NOS3</i>	$\Delta$ Ct	0.1599 ± 0.0597	0.1075 ± 0.0592	0.1686 ± 0.0643	0.2636 ± 0.0972	0.0176 ± 0.0056	0.0187 ± 0.0174	0.0170 ± 0.0060	0.0347 ± 0.0382
	fold change	1	0.67	1.05	<b>1.65</b>	1	1.06	0.97	<b>1.97</b>
	<i>p</i> -value	1.00	0.082	0.969	<b>0.001</b>	1.00	0.997	0.999	<b>0.050</b>
<i>SNAI1</i>	$\Delta$ Ct	0.0595 ± 0.0214	0.0513 ± 0.0284	0.0650 ± 0.0257	0.0943 ± 0.0377	0.0017 ± 0.0008	0.0020 ± 0.0017	0.0015 ± 0.0008	0.0031 ± 0.0024
	fold change	1	0.86	1.09	<b>1.58</b>	1	1.18	0.88	<b>1.82</b>
	<i>p</i> -value	1.00	0.728	0.892	<b>0.002</b>	1.00	0.937	0.969	<b>0.031</b>
<i>SNAI2</i>	$\Delta$ Ct	0.0162 ± 0.0088	0.0097 ± 0.0056	0.0196 ± 0.0100	0.0521 ± 0.0311	0.0003 ± 0.0003	0.0005 ± 0.0006	0.0002 ± 0.0001	0.0003 ± 0.0003
	fold change	1	0.60	1.21	<b>3.22</b>	1	1.57	0.63	1.01
	<i>p</i> -value	1.00	0.596	0.901	<b>0.001</b>	1.00	0.451	0.856	0.999
<i>TWIST1</i>	$\Delta$ Ct	0.0019 ± 0.0010	0.0016 ± 0.0009	0.0022 ± 0.0011	0.0029 ± 0.0014	0.00013 ± 0.0001	0.0002 ± 0.0001	0.0001 ± 0.0001	0.0003 ± 0.0003
	fold change	1	0.84	1.16	1.53	1	1.54	0.85	2.31
	<i>p</i> -value	1.00	0.757	0.794	0.086	1.00	0.992	0.981	0.094
<i>ZEB1</i>	$\Delta$ Ct	0.3158 ± 0.2627	0.2493 ± 0.0424	0.2738 ± 0.0783	0.2246 ± 0.2089	0.0468 ± 0.0208	0.0734 ± 0.0970	0.0227 ± 0.0064	0.0589 ± 0.0651
	fold change	1	0.16	0.23	0.71	1	1.57	0.49	1.26
	<i>p</i> -value	1.00	0.294	0.323	0.276	1.00	0.403	0.477	0.875

Note. For the analyzed genes, see note to Table 1.

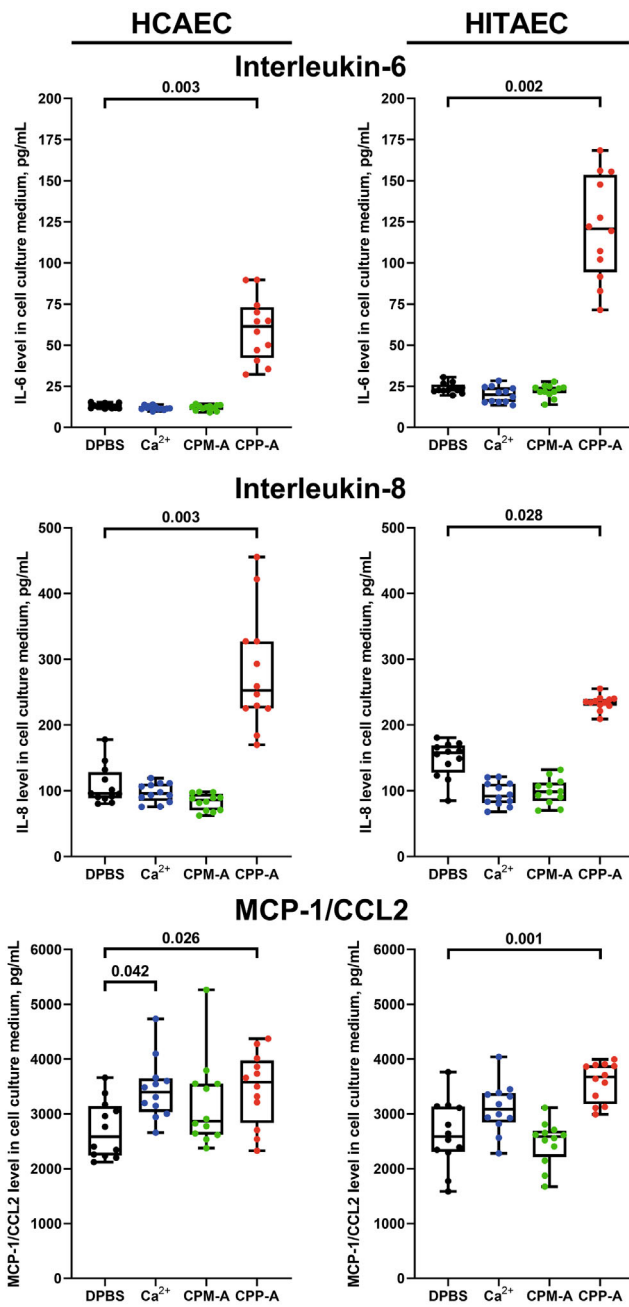


**Fig. 6.** Assessment of IL-6 (top panel), IL-8 (middle panel), and MCP-1/CCL2 (bottom panel) in non-concentrated serum-free cell culture medium from HCAECs and HITAECs treated with DPBS (control; black), free Ca<sup>2+</sup> ions (blue), CPM-A (green), and CPP-A (red) (10 µg of calcium per 1 mL of serum-free cell culture medium) for 24 h (ELISA).

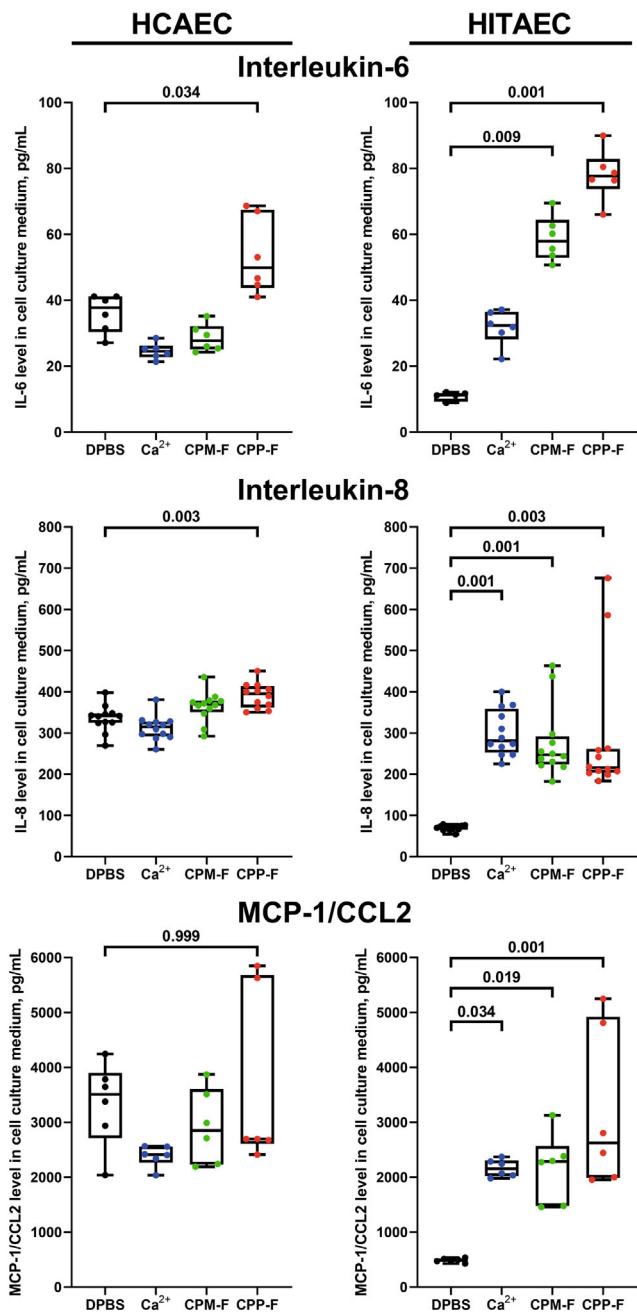


**Fig. 7.** Assessment of IL-6 (top panel), IL-8 (middle panel), and MCP-1/CCL2 (bottom panel) in non-concentrated serum-free cell culture medium from HCAECs and HITAECs treated with DPBS (control; black), free Ca<sup>2+</sup> ions (blue), CPM-F (green), and CPP-F (red) (10 µg of calcium per 1 mL of serum-free cell culture medium) for 24 h (ELISA).

and RANTES/CCL5] were upregulated after addition of CaCl<sub>2</sub> (Fig. 8 and Table S1 in the Online Resource 1). The most upregulated molecules were soluble CD147 (also called extracellular matrix metalloproteinase inducer, EMMPRIN or basigin; fold change, 11.41 in HCAECs after exposure to CPP-A) and MIP-3α/CCL20 (fold change, 12.52 in HITAECs, also after exposure to CPP-A).

Likewise, incubation of monocytes with CPP-A induced release of serpin E1/PAI-1, CXCL1/growth regulated protein alpha (GROα), chemokine (C-X-C motif) ligand 5/epithelial neutrophil-activating protein 78 (CXCL5/ENA-78), adiponectin, neutrophil gelatinase-associated lipocalin (NGAL)/lipocalin-2, IL-6, chitinase 3-like 1, apolipoprotein A-I, uPAR, MIP-3α/CCL20, and MMP-9, in contrast to Ca<sup>2+</sup> and CPM-A, which triggered

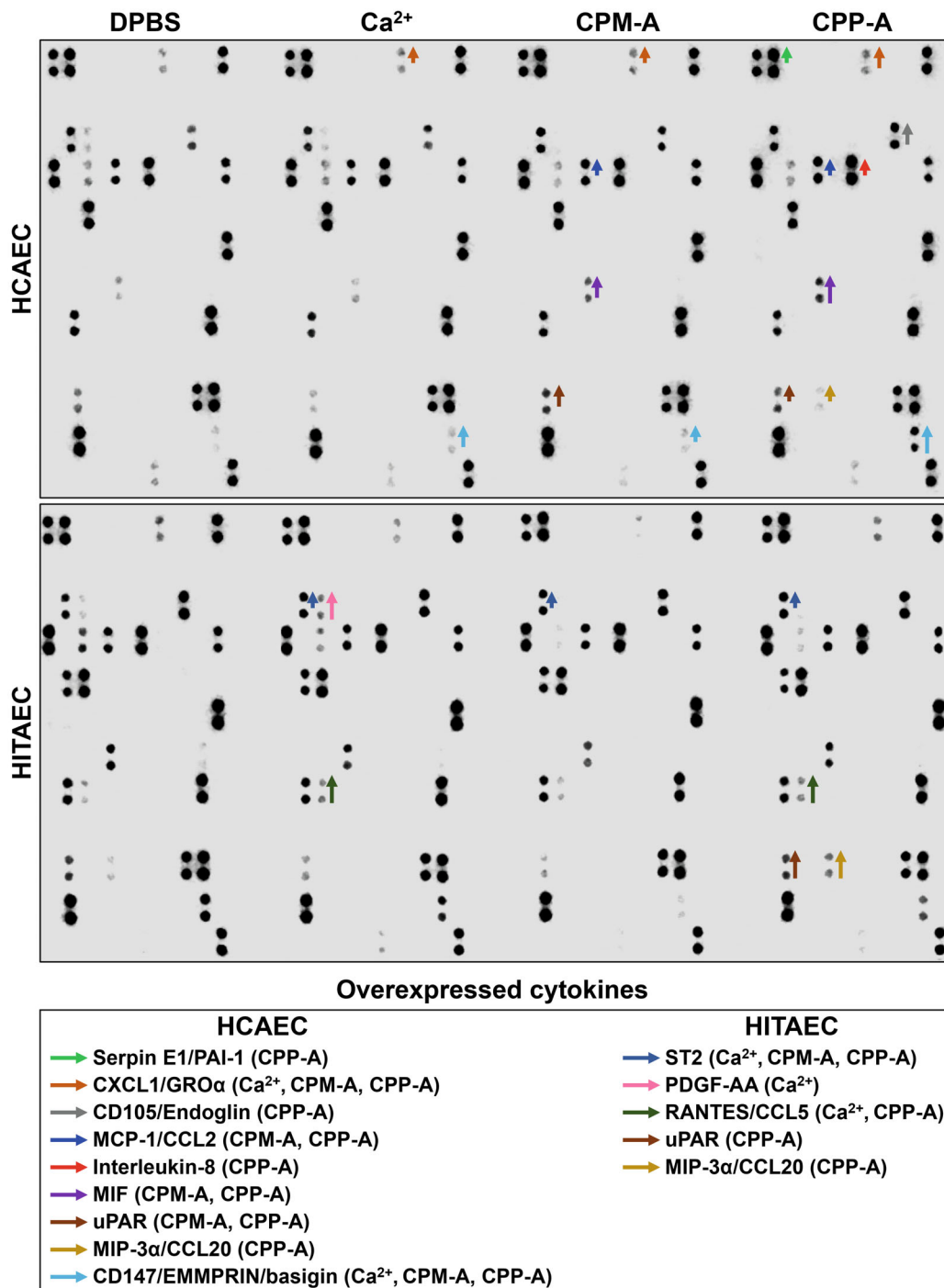


**Fig. 8.** Cytokine profiling of concentrated (3-fold) serum-free cell culture medium from HCAECs (top) and HITAECs (bottom) treated with DPBS (control), free Ca<sup>2+</sup> ions, CPM-A, or CPP-A (10  $\mu$ g of calcium per 1 mL of cell culture medium) for 24 h (dot blotting). Green, serpin E1/PAI-1; light brown, CXCL1/GRO $\alpha$ ; gray, CD105/endoglin; dark blue, MCP-1/CCL2; red, IL-8; violet, MIF; dark brown, uPAR; gold, MIP-3 $\alpha$ /CCL20; light blue, CD147/EMMPRIN/basigin; azure, ST2; pink, PDGF-AA; dark green, RANTES/CCL5. Short, medium, and long arrows indicate fold change from 1.20 to 1.49, from 1.50 to 1.99, and  $\geq 2.00$ , respectively, as compared with the DPBS group.

stochastic alterations of cytokine release (Fig. 9 and Table S2 in the Online Resource 1). CPP-A caused an increased release of eleven abovementioned cytokines into the milieu, while the effects of Ca<sup>2+</sup> and CPM-A were limited to the induction of NGAL/lipocalin-2,

chitinase 3-like 1, and MMP-9 (Fig. 9 and Table S2 in the Online Resource 1). CXCL1, adiponectin, IL-6, and apolipoprotein A-I were exclusively expressed in the monocyte-derived culture medium upon the incubation with CPP-P (amorphous primary CPPs).

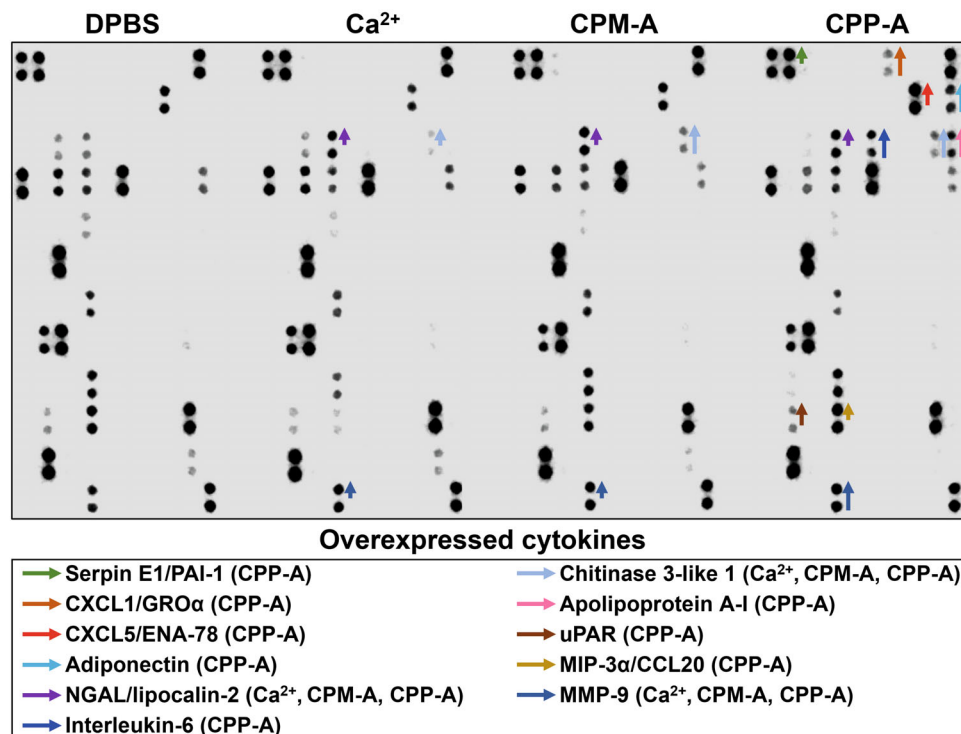


**Fig. 9.** Cytokine profiling of concentrated (7-fold) serum-free cell culture medium of human monocytes treated with DPBS (control), free Ca<sup>2+</sup> ions, CPM-A, and CPP-A (10 μg of calcium per 1 mL of cell culture medium) for 24 hours (dot blotting). Green, serpin E1/PAI-1; light brown, CXCL1/GROα; red, CXCL5/ENA-78; light blue, adiponectin; violet, NGAL/lipocalin-2; dark blue, IL-6; sky blue, chitinase 3-like 1; pink, apolipoprotein A-I; brown, uPAR; gold, MIP-3α; dark green, MMP-9. Short, medium, and long arrows indicate fold change from 1.20 to 1.49, 1.50 to 1.99, and ≥2.00, respectively, as compared with the DPBS group.

Hence, we found that CPP-A caused pro-inflammatory activation of ECs and monocytes, as evidenced by the upregulation of expression of multiple cytokine genes and increased release of corresponding proteins. Although free Ca<sup>2+</sup> ions and CPM-A also induced release of several cytokines by ECs, their pro-inflammatory effects were less pronounced as compared to CPP-A regardless of the cell line (HCAECs, HITAECS, and monocytes).

**All tested calcium delivery forms induce systemic inflammatory response in rats in the absence of other cardiovascular risk factors.** Finally, we examined *in vivo* effects of various calcium stress modalities after intravenous administration of CaCl<sub>2</sub>, CPM-A, and CPP-A to normolipidemic and normotensive Wistar rats (10 μg of calcium per 1 mL of blood). In contrast to the *in vitro* findings, all calcium delivery forms caused an elevation in the content of pro-inflammatory cytokines in rat serum as evidenced by dot blotting (22, 30, and 24 cytokines in the case of Ca<sup>2+</sup>, CPM-A, and CPP-A injections, respectively; Fig. 10 and Table S3 in the Online Resource 1). Among these molecules were granulocyte-macrophage colony-stimulating factor (GM-CSF), chemokines [chemokine (C-X3-C motif) ligand 1 (CX3CL1, fractalkine), MCP-1/CCL2, chemokine (C-X-C motif) ligand 7 (CXCL7), C-C motif

chemokine 11 (CCL11, eotaxin), C-C motif chemokine 17 (CCL17)], serpin E1/PAI-1, matrix metalloproteinase 2 (MMP-2), matrix metalloproteinase 3 (MMP-3), hepatokines [hepessocin, fetuin-A, fibroblast growth factor (FGF-21), growth/differentiation factor 15 (GDF-15)], and proteins with pleiotropic effects [receptor for advanced glycation end-products (RAGE/AGER), adiponectin, fibulin-3, galectin-1, and galectin-3] (Fig. 10 and Table S3 in the Online Resource 1).

Prolactin, GM-CSF, hepessocin, ciliary neurotrophic factor (CNTF), MMP-3, CX3CL1/fractalkine, FGF-21, fibulin-3, and GDF-15 were upregulated after all three types of calcium intervention (Fig. 10 and Table 3 in the Online Resource 1). Yet, RAGE/AGER, fetuin-A, MCP-1/CCL2, MMP-9, CCL17, and galectin-3 were upregulated exclusively after injections of CPM-A and CPP-A, while release of hepatocyte growth factor (HGF), CCL11/eotaxin, and galectin-1 was stimulated only by CPM-A; serpin E1/PAI-1 was upregulated solely by CPP-A (Fig. 10 and Table S3 in the Online Resource 1). Among the cytokines overrepresented in the cell culture medium from the CPM-A-treated ECs and monocytes, MCP-1/CCL2 and MMP-9 remained elevated in the serum of rats injected with either CPM-A or CPP-A (Table 3). The content of three proteins (uPAR, CXCL1/GROα, and MIP-3α/CCL20) was increased

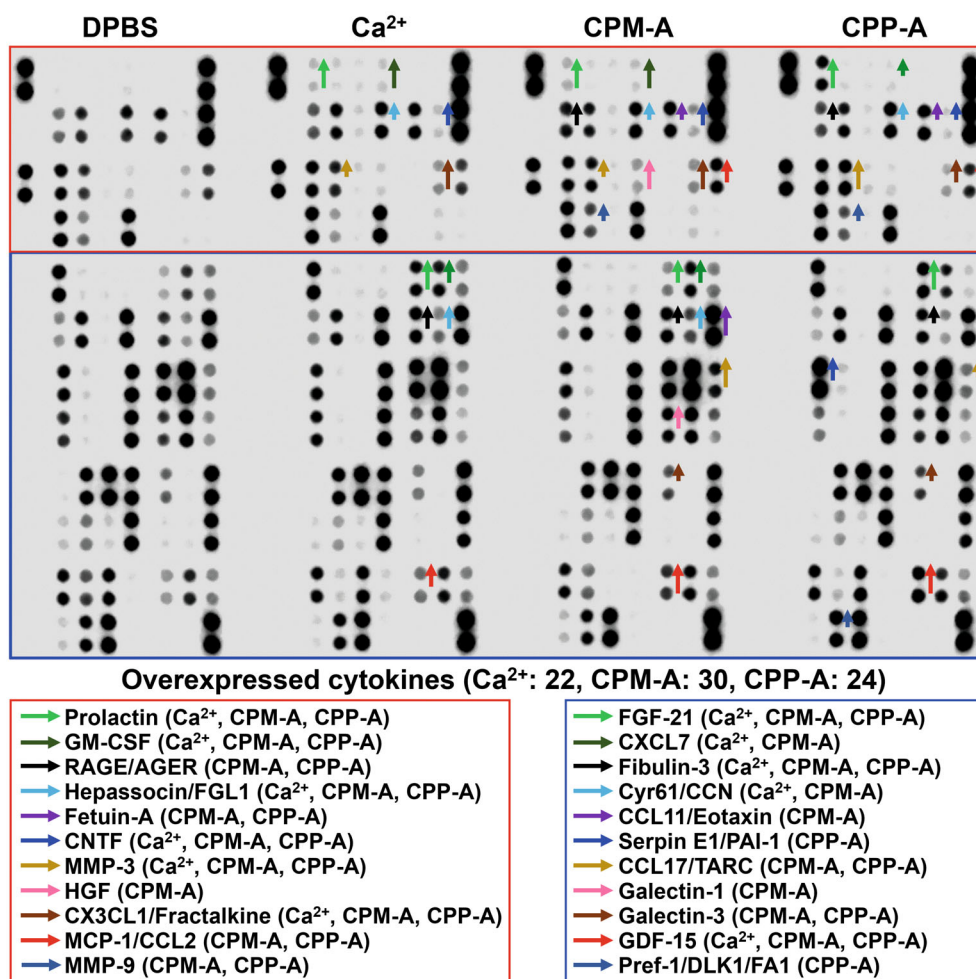


**Fig. 10.** Cytokine profiling of nonconcentrated serum from rats treated with DPBS (control), free Ca<sup>2+</sup> ions, CPM-A, and CPP-A (10 µg of calcium per 1 mL of blood) for 1 h. Top panel (red box): green, prolactin; dark green, GM-CSF; black, RAGE/AGER; light blue, hepassocin/fibrinogen-like protein 1 (FGL-1); violet, fetuin-A; dark blue, ciliary neurotrophic factor (CNTF); gold, MMP-3; pink, hepatocyte growth factor (HGF); brown, chemokine (C-X3-C motif) ligand 1 (CX3CL1)/fractalkine; red, MCP-1/CCL2; azure, MMP-9. Bottom panel (blue box): green, fibroblast growth factor 21 (FGF21); dark green, chemokine (C-X-C motif) ligand 7 (CXCL7); black, fibulin-3; light blue, cysteine-rich angiogenic inducer 61/CCN family member 1 (Cyr61/CCN1); violet, C-C motif chemokine 11 (CCL11)/eotaxin; dark blue, serpin E1/PAI-1; gold, C-C motif chemokine 17 (CCL17)/thymus and activation-regulated chemokine (TARC); pink, galectin-1; brown, galectin-3; red, growth/differentiation factor 15 (GDF-15); azure, Pref-1/delta like non-canonical Notch ligand 1 (DLK1)/fetal antigen-1 (FA1). Short, medium, and long arrows indicate fold change from 1.20 to 1.49, 1.50 to 1.99, and ≥2.00, respectively, as compared with the DPBS group.

in the cell culture medium from ECs and monocytes treated with CPP-A (Table 3). uPAR and MIP-3α/CCL20 were upregulated in the culture medium from all three types of cells (HCAECs, HITAECs, and monocytes), but not in the rat serum. Serpin E1/PAI-1 was the only molecule that was upregulated in all samples (EC- and monocyte-derived cell culture medium and rat serum) after CPP-A treatment (Table 3).

## DISCUSSION

Disturbed mineral homeostasis, e.g., reduction in serum albumin and increase in serum calcium or phosphate, is an independent cardiovascular risk fac-

tor [11]. It a manifestation of chronic kidney disease which also promotes endothelial dysfunction via elevating serum concentrations of urea and creatinine [53, 54]. In addition to these biochemical triggers, endothelial dysfunction is exacerbated by internalization of CPPs by vascular ECs [8-15] and liver sinusoidal ECs [17, 18] resulting in the development of chronic low-grade inflammation [13, 14]. CPP internalization is associated with the increased levels of pro-inflammatory cytokines, dysregulated balance between vasoconstriction and vasodilation (including decreased NO production), and endothelial-to-mesenchymal transition [55]. In particular, internalization of CPPs by ECs and monocytes triggers the release of inducible endothelial cytokines (IL-6, IL-8, MCP-1/CCL2, and soluble

**Table 3.** Specific and common cytokines elevated in EC- or monocyte-derived cell culture medium or rat serum upon the treatment with free Ca<sup>2+</sup> ions, CPM-A, and CPP-A (10 µg of calcium per 1 mL of cell culture medium or blood) for 24 h (cells) or 1 h (rats) compared with the control (DPBS)

Calcium stress inducer	<i>In vitro</i> (serum-free culture medium from HCAECs and HITAECs)	<i>In vitro</i> (serum-free culture medium from monocytes)	<i>In vivo</i> (rat serum)
Free Ca <sup>2+</sup> ions delivered by CaCl <sub>2</sub>	CXCL1/GROα, CD147/EMMPRIN/basigin, ST2, PDGF-AA, MIP-3α/CCL20	NGAL/lipocalin-2, chitinase 3-like 1, MMP-9	prolactin, GM-CSF, hepassocin/FGL1, CNTF, MMP-3, CX3CL1/fractalkine, FGF-21, CXCL7, fibulin-3, Cyr61/CCN, GDF-15
CPM-A	MCP-1/CCL2, CXCL1/GROα, MIF, uPAR, CD147/EMMPRIN/basigin, ST2	MMP-9, NGAL/lipocalin-2, chitinase 3-like 1	MCP-1/CCL2, MMP-9, prolactin, GM-CSF, RAGE/AGER, hepassocin/FGL1, fetuin-A, CNTF, MMP-3, HGF, CX3CL1/fractalkine, FGF-21, CXCL7, fibulin-3, Cyr61/CCN, CCL11/eotaxin, CCL17/TARC, galectin-1, galectin-3, GDF-15
CPP-A	Serpin E1/PAI-1, uPAR, CXCL1/GROα, MIP-3α/CCL20, MCP-1/CCL2, CD105/endoglin, IL-8, MIF, CD147/EMMPRIN/basigin, ST2, RANTES/CCL5	Serpin E1/PAI-1, uPAR, CXCL1/GROα, MIP-3α/CCL20, MMP-9, CXCL5/ENA-78, adiponectin, NGAL/lipocalin-2, IL-6, chitinase 3-like 1, apolipoprotein A-I	Serpin E1/PAI-1, MCP-1/CCL2, MMP-9, prolactin, GM-CSF, RAGE/AGER, hepassocin/FGL1, fetuin-A, CNTF, MMP-3, CX3CL1/fractalkine, FGF-21, fibulin-3, CCL17/TARC, galectin-3, GDF-15, Pref-1/DLK1/FA1
CPM-A: upregulated in ECs and rats	MCP-1/CCL2		
CPM-A: upregulated in monocytes and rats	MMP-9		
CPP-A: upregulated in ECs and monocytes	uPAR, CXCL1/GROα, MIP-3α/CCL20		
CPP-A: upregulated in ECs and rats	MCP-1/CCL2		
CPP-A: upregulated in monocytes and rats	MMP-9		
CPP-A: upregulated in ECs, monocytes, and rats	Serpin E1/PAI-1		

intercellular adhesion molecule sICAM-1) and monocyte-derived cytokines [MIP-1α, MIP-3α, cytokine-induced neutrophil chemoattractant-1 (CINC-1), cytokine-induced neutrophil chemoattractant-3 (CINC-3), and C-X-C motif chemokine ligand 10 (CXCL10)] [13]. Since chronic low-grade inflammation and endothelial

dysfunction mutually promote each other [56-59], it is difficult to distinguish the contribution of CPP-stimulated ECs and monocytes, as well as specific cytokines produced by these cells, to systemic inflammation.

According to the recent concepts, nanometer-sized (~9-10 nm) CPMs act as building blocks for

submicrometer-sized (~30-100 nm) primary CPPs (or CPP-I), which, in turn, undergo aggregation and amorphous-to-crystalline transition to micrometer-sized (100-300 nm) secondary CPPs (or CPP-II) [18, 27, 60, 61]. Initially amorphous and spherical, primary CPPs mature into spindle- or needle-shaped crystalline secondary CPPs [18, 27, 60, 61]. While CPMs and primary CPPs consist of amorphous calcium phosphate, secondary CPPs are composed of carbonate hydroxyapatite, also called bioapatite. All these calcium and phosphate scavengers can adsorb proteins from the surrounding medium (e.g., circulating proteins from the blood) [18, 27, 60, 61]. Calcium and phosphate react with each other in the presence of the mineral chaperone fetuin-A and other acidic serum proteins with the formation of amorphous calcium phosphate (CPMs or primary CPPs) or carbonate hydroxyapatite (secondary CPPs) [22, 62-64]. CPPs act as mineral scavengers; phosphate as an inherent component of hydroxyapatite is an essential constituent of these compounds [22, 62-64]. It was reported that high phosphate concentrations inhibit production of nitric oxide, thus impairing vasodilation [65-67], induce apoptosis of endothelial cells [65, 67], and promote systemic inflammation in a dose-dependent manner by triggering oxidative stress and stimulating expression of pro-inflammatory cytokines [68]. Hence, high phosphate is considered as an independent factor of endothelial dysfunction and chronic low-grade inflammation [69-71].

Although it has been shown that exhaustion of the serum  $\text{Ca}^{2+}$ -binding capacity leads to the precipitation of CPPs and that mineral stress affects the development of endothelial dysfunction and systemic inflammation, it remained unclear whether the consequences of calcium overload are solely determined by the calcium amount or also by the form of calcium delivery (free  $\text{Ca}^{2+}$  ions, CPMs, and CPPs). Typically, CPMs and CPPs are generated artificially by combining excessive concentrations of calcium and phosphate with a protein source in a buffering solution. The above question can be answered by applying a holistic approach (by adding serum as a protein source) or a reductionist approach (by adding a major serum protein, e.g., albumin or fetuin-A, as a protein source). The holistic approach recapitulates a scenario occurring in human serum, while the reductionist approach allows to analyze the mineral-buffering capacity of each serum protein and to avoid potential negative effects of other serum components. To better address the task of modeling mineral stress, here we applied the reductionist approach to synthesize simultaneously CPMs and CPPs. We chose BSA as a protein source for CPM-A and CPP-A because (i) the lower quartile of serum albumin content is associated with cardiovascular disease and correlates with increased serum calcification propensity [11]; (ii) the concentration of

serum albumin positively correlates with the concentration of serum CPPs (measured with fluorescently labeled bisphosphonate) and total calcium [11]; (iii) albumin represents one of the two primary scavengers of ionized calcium along with fetuin-A [7]; (iv) albumin is convenient to use as its yellow color facilitates visual quality control. Beside BSA, we also used BSF to synthesize CPM-F and CPP-F because fetuin-A is a primary mineral chaperone that maintains generation of CPMs and CPPs in human body [1-4].

When physiological concentrations of BSA were mixed with supraphysiological concentrations of calcium and phosphate, the ratio (%) between the ionized, protein-bound (CPMs), and phosphate-bound (CPPs) calcium was 50 : 20 : 30, respectively. This validated the physiological relevance of the implemented mineral stress model (as the distribution of ionized to bound calcium was 1 : 1) and confirmed that circulating mineral depots – CPMs and CPPs – are able to maintain their calcium-binding function at the physiological level even upon severe mineral stress. During mineral stress, the amount of calcium in CPPs exceeded that in CPMs, thus highlighting the primary role of CPPs as mineral scavengers buffering the human blood and controlling the level of ionized calcium. These results are in accordance with the earlier reports on the calcium ratio in CPPs and CPMs (1 : 1) [18, 72]. They suggest that CPPs represent an ultimate buffer that aggregates excessive calcium and phosphate to prevent blood supersaturation with ionized calcium when other mineral buffers are exhausted. A relatively low proportion of albumin bound to CPPs (~15%) even at supraphysiological conditions of mineral stress indicated that CPP generation, probably, does not affect the functions of albumin in a living organism.

To compare the effects of different calcium vehicles ( $\text{CaCl}_2$  as a donor of  $\text{Ca}^{2+}$  ions, CPM-A/CPM-F, and CPP-A/ CPP-F), we selected ECs and monocytes, which are the first cell populations encountering CPPs in an organism. In this study, we determined and used the physiological dose of calcium (10  $\mu\text{g}/\text{mL}$ ), as this parameter is strictly regulated in a body in order to prevent arrhythmia and extraskeletal calcification [73-75]. This dose induced a 10% increase in the ionized calcium concentration, which corresponded to the interquartile range of plasma ionized calcium in the population (from 0.10 to 0.14 mmol/L, i.e., from 4.0 to 5.6  $\mu\text{g}/\text{mL}$ ) [11]. Internalization of CPPs is a mandatory pre-requisite of their detrimental effects [8-19]. We showed that CPMs are internalized by the ECs in a flow similarly to CPPs [10, 13]. In accordance with our previous findings [9-15], incubation of arterial ECs with CPP-A upregulated expression of genes encoding pro-inflammatory cell adhesion molecules (*VCAM1*, *ICAM1*, and *SELE*) and pro-inflammatory cytokines (*IL6*, *CXCL8*, *CCL2*, and *CXCL1*). The treatment

of arterial ECs with CPP-F promoted expression of *VCAM1*, *ICAM1*, *SELE*, *SELP*, *IL6*, *MIF*, and *CXCL1* genes. Such molecular reconfiguration is typical for dysfunctional ECs [55, 76, 77] and indicates development of chronic low-grade inflammation [56-59] and senescence-associated secretory phenotype [78-80].

Incubation of ECs and monocytes with CPP-A or CPP-F (10  $\mu$ g of calcium per 1 mL of cell culture medium) promoted release of pro-inflammatory cytokines. Among the molecules upregulated in arterial ECs and monocytes after their exposure to CPP-A were cytokines and chemokines (IL-6, IL-8, MCP-1/CCL2, CXCL1/GRO $\alpha$ , MIP-3 $\alpha$ /CCL20), as well as pro- and anti-thrombotic molecules (serpin E1/PAI-1 and uPAR). Of these, uPAR, MIP-3 $\alpha$ /CCL20, and serpin E1/PAI-1 were consistently upregulated in HCAECs, HITAECs, and monocytes. To summarize the results of *in vitro* experiments, exposure to CPPs triggered the pro-inflammatory response characterized by the activation of cytokine release and corresponding changes in the gene expression. Although Ca<sup>2+</sup>, CPM-A, and CPM-F also stimulated production of several cytokines by ECs, this response was less pronounced and suggested limited pathogenic effects of these calcium sources.

Cytokine profiling by ELISA revealed a statistically significant elevation in the IL-6, IL-8, and MCP-1/CCL2 production by both HCAECs and HITAECs after their incubation with CPP-A. Yet, dot blot experiments found an increase in the IL-8 and MCP-1/CCL2 content exclusively in HCAECs; no IL-6 was detected in the cell culture supernatant even after concentrating it 3-fold. The most probable reason for this discrepancy is a limited sensitivity of semi-quantitative chemiluminescent dot blotting, as IL-6 levels did not exceed 175 pg/mL (in comparison with 250-500 pg/mL for IL-8 and 2500-6000 pg/mL for MCP-1/CCL2). This suggestion was partially confirmed in our previous study [13], in which the concentration of IL-6 after 24-hour culturing of CPP-treated ECs reached 300-450 pg/mL and could be detected by dot blotting.

Previous studies consistently reported cytotoxic and pro-inflammatory (primarily NLRP3 inflammasome-mediated) effects of CPPs mediated by the calcium and osmotic stress that resulted from a sharp rise in the cytosolic Ca<sup>2+</sup> following the dissolution of calcium in the lysosomes [11, 81, 82]. Bafilomycin A1, a specific inhibitor of vacuolar H<sup>+</sup> ATPase (V-ATPase), rescued ECs [11] and vascular smooth muscle cells [81] from the CPP-induced lysosome-dependent cell death by preventing lysosomal acidification and CPP dissolution. Similar cytoprotective effects were reached by using inhibitors of calcium-sensing receptor NLRP3 or caspase-1 during the calcium stress [82]. Likewise, pharmacological inhibition of cathepsin B, a prominent lysosomal protease, ameliorated the CPP-related release of IL-1 $\beta$  by the macrophages [25, 82].

Gene set enrichment analysis revealed an upregulation of lysosome-related proteins, in particular, lysosomal membrane proteins, in arterial ECs [13]. Moreover, molecular terms related to the lysosome-mediated calcium dissolution (e.g., vacuolar acidification, pH regulation, regulation of proteolysis, Ca<sup>2+</sup> elevation in cytosol, and mitochondrial outer membrane permeabilization) were also upregulated in CPP-treated HCAECs and HITAECs [13]. Further proteomic analysis suggested that lysosomal response to CPP internalization involves pre-existing protein machinery rather than employs transcriptional, post-transcriptional, and translational regulation [15]. Although some studies reported lysosomal alkalization and reduced hydrolase activity during CPP dissolution because of Ca<sup>2+</sup> overflow [26, 28], here we were able to detect CPP-A and CPP-F in EC lysosomes using standard pH sensor (LysoTracker Red). Taken together lysosome-specific distribution and cytotoxic and pro-apoptotic effects of CPP-A and CPP-F, we suggested that their pathogenic profile is similar to those of atherosclerotic plaque- and serum-derived CPPs [8], as well as to CPP-P and CPP-S (crystalline secondary CPPs) [9-13, 15].

Intravenous administration of Ca<sup>2+</sup>, CPM-A, or CPP-A to Wistar rats free of other cardiovascular risk factors, also triggered systemic inflammatory response primarily mediated by chemokines (MCP-1/CCL2, CX3CL1, CXCL7, CCL11, and CCL17), hepatokines (hepaticin, fetuin-A, FGF-21, and GDF-15), proteases (MMP-2 and MMP-3), and protease inhibitors (serpin E1/PAI-1). Hence, our *in vitro* and *in vivo* findings supported a pronounced pro-inflammatory effect of CPPs. For this study, we selected a 1-hour time point based on the results of our previous works [13] and taking into account rapid utilization of excessive calcium from the blood through its clearance by acidic serum proteins acting as Ca<sup>2+</sup> scavengers, removal of CPMs by kidneys, and recycling of CPPs in the liver [5]. Notably, ionized calcium concentration represents one of the most tightly regulated biochemical parameters in the human blood (which can even be compared to pH), as stable hypercalcemia is a relatively rare condition and even transient hypercalcemia might lead to arrhythmia [83-86]. Hence, the model of transient hypercalcemia, a condition that frequently occurs in patients with hyperparathyroidism or excessive vitamin D intake, is quite relevant [83-86]. The pathological effects of calcium stress observed 1 h after the intravenous administration of CaCl<sub>2</sub>, CPMs, or CPPs to Wistar rats, were related to the low-grade systemic inflammation defined as a minor to moderate increase in the cytokine levels in the circulation. Such calcium stress-derived transient increase leads to a pro-inflammatory state which might negatively affect vascular health by sustaining endothelial activation. If uncurbed (e.g., in elderly patients having more than one comorbid

condition, such as diabetes mellitus or chronic kidney disease), these transient elevations of pro-inflammatory cytokines can contribute to the frailty syndrome, in which biological age (i.e., age-related functional decline) exceeds the chronological age [56-59].

Our results are in agreement with the data obtained by Wilhelm Jahnén-Dechent's group, who showed the absence of CPM toxicity or pro-inflammatory effects after internalization by sinusoidal liver ECs and proximal tubular epithelial cells, in contrast to CPPs, which exhibited significant cytotoxic effects and triggered rapid assembly of NLRP3 inflammasome as early as within 2 h after CPP addition [18]. Combined analysis of *in vitro* and *in vivo* results revealed that serpin E1/PAI-1 was the only molecule upregulated in ECs, monocytes, and rat serum after CPP-A treatment. The reasons behind this stable upregulation of serpin E1/PAI-1 might include its relative abundance (which permits to detect and increase in its release by dot blotting) and calcium-dependent regulation. Other cytokines overrepresented in the cell culture supernatant from the CPP-A/ CPP-F-treated ECs or monocytes or in the serum of CPP-A/ CPP-F-treated rats (uPAR, CXCL1/GRO $\alpha$ , MIP-3 $\alpha$ /CCL20, MCP-1/CCL2, and MMP-9) exhibited less consistent expression across the experimental models. For instance, uPAR and CXCL1/GRO $\alpha$  produced only a moderate signal in the cell culture supernatant from either ECs or monocytes, while MIP-3 $\alpha$ /CCL20 and MMP-9 were highly expressed in monocytes but not in the control ECs. Similar to serpin E1/PAI-1, MCP-1/CCL2 showed a relatively high expression in all models but was not upregulated in monocytes. Further, serpin E1/PAI-1 is produced [87, 88] and even its activity is maintained [89] in a calcium-dependent manner, suggesting an existence of a mechanism ensuring activation of its release after the treatment with CPP-A or CPP-F. Unfortunately, previous studies have not examined production of serpin E1/PAI-1 by the cell populations after exposure to CPPs.

Future studies might further investigate the effects of CPMs and CPPs, considering a higher affinity of fetuin-A for calcium and a unique function of this protein as a mineral chaperone governing the CPP formation, although the average fetuin-A level in the serum (1 g/L) is significantly lower than that of albumin (34 g/L) [90-93]. It might be promising to investigate combined effects of Ca<sup>2+</sup> and CPMs or CPPs, as Ca<sup>2+</sup>-dependent calcium-sensing receptor promotes internalization of CPPs [39], which might exacerbate their pathogenic effects. Another task is to define the hierarchy in the mineral-binding ability of acidic serum proteins (albumin, fetuin-A, osteonectin, osteoprotegerin, osteopontin, matrix Gla protein, Gla-rich protein, alpha-1-acid glycoprotein, transferrin, haptoglobin, fibrinogen, ceruloplasmin, alpha-2-macroglobulin, immunoglobulin A, fibronectin, and antithrom-

bin III). From the diagnostic viewpoint, differential detection of CPMs and CPPs might be performed using the flow cytometry approach with fluorescently labeled bisphosphonate (e.g., IVISense Osteo 680) and artificially synthesized CPMs and CPPs used to set the CPM- and CPP-specific gates. Measuring serum concentrations of CPMs and CPPs in healthy individuals and in various diseases states might help to better understand the pathophysiological importance of these parameters.

Our findings suggest that the adverse effects of calcium stress are determined by the calcium delivery mode rather than simply by the amount of calcium. This might indicate the necessity to reconsider the approaches for CPP quantification, albeit alternative techniques (fluorescent labeling in combination with flow cytometry, turbidimetry, nephelometry, dynamic light scattering, and scanning electron microscopy) are less standardized and their application for CPP quantification *in vitro* is currently debated. Dynamic light scattering and scanning electron microscopy are time-consuming, while turbidimetry depends on the particle-size distribution. Apparently, future studies will need to address the development of new methods for CPP quantification.

## CONCLUSIONS

We found that physiological increase in the Ca<sup>2+</sup> concentration (by 10%, which is equal to the interquartile range in a population) was achieved by adding 10  $\mu$ g of calcium to 1 mL of serum-free medium or rat serum. Incubation of ECs and monocytes with such amount of CPP-A or CPP-F initiated their pro-inflammatory activation that was manifested as transcriptional reprogramming and increased release of endothelium-derived (IL-6, IL-8, MCP-1/CCL2, uPAR, MIP-3 $\alpha$ /CCL20, serpin E1/PAI-1) and monocyte-derived (IL-6, IL-8, MIP-1 $\alpha$ /1 $\beta$ , MIP-3 $\alpha$ /CCL20, uPAR, serpin E1/PAI-1, CXCL1, CXCL5) cytokines. Addition of free Ca<sup>2+</sup> and CPM-A induced limited detrimental effects in ECs and monocytes, although CPMs were internalized by ECs in a flow similar to CPPs. All forms of calcium delivery (free Ca<sup>2+</sup> ions, colloidal CPM-A, and corpuscular CPP-A) caused systemic inflammatory response in normolipidemic and normotensive Wistar rats (Ca<sup>2+</sup>: 22 cytokines, CPM-A: 30 cytokines, CPP-A: 24 cytokines). Serpin E1/PAI-1 was the only molecule upregulated in all tested cells (ECs and monocytes) and rat serum after the treatment with CPP-A. The increase in the release of chemokines (CX3CL1, MCP-1/CCL2, CXCL7, CCL11, CCL17) and hepatokines (hepatocin, fetuin-A, FGF-21, GDF-15) at the background of upregulated cytokine expression suggested chemokine burst and release of liver injury markers.

**Supplementary information.** The online version containing supplementary material is available at <https://doi.org/10.1134/S0006297924604064>.

**Contributions.** Conceptualization, D.Sh. and A.K. developed the study concept and performed data validation; D.Sh., Victoria M., Yu.M., M.S., A.S., Vera M., E.T., A.L., and A.S. developed the methodology, performed the experiments, and analyzed the data; A.K. analyzed and curated the data, acquired the funding, supervised the project, prepared the figures, wrote and edited the text of the article. All authors have read and agreed to the published version of the manuscript.

**Funding.** This study was funded by the Russian Science Foundation (project no. 22-15-00107 “Circulation of calciprotein particles in human blood: pathogenic consequences and molecular mechanisms” to A.K.; <https://rscf.ru/en/project/22-15-00107/>).

**Ethics approval and consent to participate.** All animal study protocols were approved by the Local Ethical Committee of the Research Institute for Complex Issues of Cardiovascular Diseases (protocol code: 042/2023; date of approval, April 4, 2023). All animal experiments were performed in accordance with the European Convention for the Protection of Vertebrate Animals (Strasbourg, 1986) and Directive 2010/63/EU of the European Parliament on the protection of animals used for scientific purposes.

**Conflict of interest.** The authors of this work declare that they have no conflict of interest.

## REFERENCES

1. Heiss, A., Pipich, V., Jahnen-Dechent, W., and Schwahn, D. (2010) Fetuin-A is a mineral carrier protein: small angle neutron scattering provides new insight on Fetuin-A controlled calcification inhibition, *Biophys. J.*, **99**, 3986-3995, <https://doi.org/10.1016/j.bpj.2010.10.030>.
2. Jahnen-Dechent, W., Heiss, A., Schäfer, C., and Kettler, M. (2011) Fetuin-A regulation of calcified matrix metabolism, *Circ. Res.*, **108**, 1494-1509, <https://doi.org/10.1161/CIRCRESAHA.110.234260>.
3. Jahnen-Dechent, W., Büscher, A., Köppert, S., Heiss, A., Kuro-O, M., and Smith, E. R. (2020) Mud in the blood: the role of protein-mineral complexes and extracellular vesicles in biomineralisation and calcification, *J. Struct. Biol.*, **212**, 107577, <https://doi.org/10.1016/j.jsb.2020.107577>.
4. Smith, E. R., Hewitson, T. D., and Jahnen-Dechent, W. (2020) Calciprotein particles: mineral behaving badly? *Curr. Opin. Nephrol. Hypertens.*, **29**, 378-386, <https://doi.org/10.1097/MNH.0000000000000609>.
5. Kutikhin, A. G., Feenstra, L., Kostyunin, A. E., Yuzhalin, A. E., Hillebrands, J. L., and Krenning, G. (2021) Calciprotein particles: balancing mineral homeostasis and vascular pathology, *Arterioscler. Thromb. Vasc. Biol.*, **41**, 1607-1624, <https://doi.org/10.1161/atvbaha.120.31569>.
6. Jahnen-Dechent, W., and Pasch, A. (2023) Solving the insoluble: calciprotein particles mediate bulk mineral transport, *Kidney Int.*, **103**, 663-665, <https://doi.org/10.1016/j.kint.2023.01.011>.
7. Bäck, M., Aranyi, T., Cancela, M. L., Carracedo, M., Conceição, N., Leftheriotis, G., Macrae, V., Martin, L., Nitschke, Y., Pasch, A., Quaglino, D., Rutsch, F., Shanahan, C., Sorribas, V., Szeri, F., Valdivielso, P., Vanakker, O., and Kempf, H. (2019) Endogenous calcification inhibitors in the prevention of vascular calcification: a consensus statement from the COST Action EuroSoftCalcNet, *Front. Cardiovasc. Med.*, **5**, 196, <https://doi.org/10.3389/fcvm.2018.00196>.
8. Kutikhin, A. G., Velikanova, E. A., Mukhamadiyarov, R. A., Glushkova, T. V., Borisov, V. V., Matveeva, V. G., Antonova, L. V., Filip'ev, D. E., Golovkin, A. S., Shishkova, D. K., Burago, A. Y., Frolov, A. V., Dolgov, V. Y., Efimova, O. S., Popova, A. N., Malysheva, V. Y., Vladimirov, A. A., Sozinov, S. A., Ismagilov, Z. R., Russakov, D. M., Lomzov, A. A., Pysnyi, D. V., Gutakovsky, A. K., Zhivodkov, Y. A., Demidov, E. A., Peltek, S. E., Dolganyuk, V. F., Babich, O. O., Grigoriev, E. V., Brusina, E. B., Barbarash, O. L., and Yuzhalin, A. E. (2016) Apoptosis-mediated endothelial toxicity but not direct calcification or functional changes in anti-calcification proteins defines pathogenic effects of calcium phosphate bions, *Sci. Rep.*, **6**, 27255, <https://doi.org/10.1038/srep27255>.
9. Shishkova, D., Velikanova, E., Sinitsky, M., Tsepokina, A., Gruzdeva, O., Bogdanov, L., and Kutikhin, A. (2019) Calcium phosphate bions cause intimal hyperplasia in intact aortas of normolipidemic rats through endothelial injury, *Int. J. Mol. Sci.*, **20**, 5728, <https://doi.org/10.3390/ijms20225728>.
10. Shishkova, D., Markova, V., Sinitsky, M., Tsepokina, A., Velikanova, E., Bogdanov, L., Glushkova, T., and Kutikhin, A. (2020) Calciprotein particles cause endothelial dysfunction under flow, *Int. J. Mol. Sci.*, **21**, 8802, <https://doi.org/10.3390/ijms21228802>.
11. Shishkova, D. K., Velikanova, E. A., Bogdanov, L. A., Sinitsky, M. Y., Kostyunin, A. E., Tsepokina, A. V., Gruzdeva, O. V., Mironov, A. V., Mukhamadiyarov, R. A., Glushkova, T. V., Krivkina, E. O., Matveeva, V. G., Hryachkova, O. N., Markova, V. E., Dyleva, Y. A., Belik, E. V., Frolov, A. V., Shabaev, A. R., Efimova, O. S., Popova, A. N., Malysheva, V. Y., Kolmykov, R. P., Sevostyanov, O. G., Russakov, D. M., Dolganyuk, V. F., Gutakovsky, A. K., Zhivodkov, Y. A., Kozhukhov, A. S., Brusina, E. B., Ismagilov, Z. R., Barbarash, O. L., Yuzhalin, A. E., and Kutikhin, A. G. (2021) Calciprotein particles link disturbed mineral homeostasis with cardiovascular disease by causing endothelial dysfunction and vascular inflammation, *Int. J. Mol. Sci.*, **22**, 12458, <https://doi.org/10.3390/ijms222212458>.

12. Bogdanov, L., Shishkova, D., Mukhamadiyarov, R., Velikanova, E., Tsepokina, A., Terekhov, A., Koshelev, V., Kanonykina, A., Shabaev, A., Frolov, A., Zagorodnikov, N., and Kutikhin, A. (2022) Excessive adventitial and perivascular vascularisation correlates with vascular inflammation and intimal hyperplasia, *Int. J. Mol. Sci.*, **23**, 12156, <https://doi.org/10.3390/ijms232012156>.
13. Shishkova, D., Lobov, A., Zainullina, B., Matveeva, V., Markova, V., Sinitskaya, A., Velikanova, E., Sinitsky, M., Kanonykina, A., Dyleva, Y., and Kutikhin, A. (2022) Calciprotein particles cause physiologically significant pro-inflammatory response in endothelial cells and systemic circulation, *Int. J. Mol. Sci.*, **23**, 14941, <https://doi.org/10.3390/ijms232314941>.
14. Feenstra, L., Kutikhin, A. G., Shishkova, D. K., Buikema, H., Zeper, L. W., Bourgonje, A. R., Krenning, G., and Hillebrands, J. L. (2023) Calciprotein particles induce endothelial dysfunction by impairing endothelial nitric oxide metabolism, *Arterioscler. Thromb. Vasc. Biol.*, **43**, 443-455, <https://doi.org/10.1161/ATVBAHA.122.318420>.
15. Shishkova, D., Lobov, A., Repkin, E., Markova, V., Markova, Y., Sinitskaya, A., Sinitsky, M., Kondratiev, E., Torgunakova, E., and Kutikhin, A. (2023) Calciprotein particles induce cellular compartment-specific proteome alterations in human arterial endothelial cells, *J. Cardiovasc. Dev. Dis.*, **11**, 5, <https://doi.org/10.3390/jcdd111010005>.
16. Herrmann, M., Schäfer, C., Heiss, A., Gräber, S., Kinkeldey, A., Büscher, A., Schmitt, M. M., Bornemann, J., Nimmerjahn, F., Herrmann, M., Helming, L., Gordon, S., and Jahnen-Dechent, W. (2012) Clearance of fetuin-A-containing calciprotein particles is mediated by scavenger receptor-A, *Circ. Res.*, **111**, 575-584, <https://doi.org/10.1161/CIRCRESAHA.111.261479>.
17. Köppert, S., Büscher, A., Babler, A., Ghallab, A., Buhl, E. M., Latz, E., Hengstler, J. G., Smith, E. R., and Jahnen-Dechent, W. (2018) Cellular clearance and biological activity of calciprotein particles depend on their maturation state and crystallinity, *Front. Immunol.*, **9**, 1991, <https://doi.org/10.3389/fimmu.2018.01991>.
18. Koeppert, S., Ghallab, A., Peglow, S., Winkler, C. F., Graeber, S., Büscher, A., Hengstler, J. G., and Jahnen-Dechent, W. (2021) Live imaging of calciprotein particle clearance and receptor mediated uptake: role of calciprotein monomers, *Front. Cell Dev. Biol.*, **9**, 633925, <https://doi.org/10.3389/fcell.2021.633925>.
19. Zeper, L. W., Bos, C., Leermakers, P. A., Franssen, G. M., Raavé, R., Hoenderop, J. G. J., and de Baaij, J. H. F. (2024) Liver and spleen predominantly mediate calciprotein particle clearance in a rat model of chronic kidney disease, *Am. J. Physiol. Renal Physiol.*, **326**, F622-F634, <https://doi.org/10.1152/ajprenal.00239.2023>.
20. Hutcheson, J. D., and Goettsch, C. (2023) Cardiovascular calcification heterogeneity in chronic kidney disease, *Circ. Res.*, **132**, 993-1012, <https://doi.org/10.1161/CIRCRESAHA.123.321760>.
21. Sutton, N. R., Malhotra, R., St Hilaire, C., Aikawa, E., Blumenthal, R. S., Gackebach, G., Goyal, P., Johnson, A., Nigwekar, S. U., Shanahan, C. M., Towler, D. A., Wolford, B. N., and Chen, Y. (2023) Molecular mechanisms of vascular health: insights from vascular aging and calcification, *Arterioscler. Thromb. Vasc. Biol.*, **43**, 15-29, <https://doi.org/10.1161/ATVBAHA.122.317332>.
22. Turner, M. E., Beck, L., Hill Gallant, K. M., Chen, Y., Moe, O. W., Kuro-O, M., Moe, S. M., and Aikawa, E. (2024) Phosphate in cardiovascular disease: from new insights into molecular mechanisms to clinical implications, *Arterioscler. Thromb. Vasc. Biol.*, **44**, 584-602, <https://doi.org/10.1161/ATVBAHA.123.319198>.
23. Smith, E. R., Hanssen, E., McMahon, L. P., and Holt, S. G. (2013) Fetuin-A-containing calciprotein particles reduce mineral stress in the macrophage, *PLoS One*, **8**, e60904, <https://doi.org/10.1371/journal.pone.0060904>.
24. Peng, H. H., Wu, C. Y., Young, D., Martel, J., Young, A., Ojcius, D. M., Lee, Y. H., and Young, J. D. (2013) Physicochemical and biological properties of biomimetic mineralo-protein nanoparticles formed spontaneously in biological fluids, *Small*, **9**, 2297-2307, <https://doi.org/10.1002/sml.201202270>.
25. Anzai, F., Karasawa, T., Komada, T., Yamada, N., Miura, Y., Sampilvanjil, A., Baatarjav, C., Fujimura, K., Matsumura, T., Tago, K., Kurosu, H., Takeishi, Y., Kuro-O, M., and Takahashi, M. (2021) Calciprotein particles induce IL-1 $\beta$ / $\alpha$ -mediated inflammation through NLRP3 inflammasome-dependent and -independent mechanisms, *Immunohorizons*, **5**, 602-614, <https://doi.org/10.4049/immunohorizons.2100066>.
26. Murthy, S., Karkossa, I., Schmidt, C., Hoffmann, A., Hagemann, T., Rothe, K., Seifert, O., Anderegg, U., von Bergen, M., Schubert, K., and Rossol, M. (2022) Danger signal extracellular calcium initiates differentiation of monocytes into SPP1/osteopontin-producing macrophages, *Cell Death Dis.*, **13**, 53, <https://doi.org/10.1038/s41419-022-04507-3>.
27. Tiong, M. K., Smith, E. R., Toussaint, N. D., Al-Khayyat, H. F., and Holt, S. G. (2021) Reduction of calciprotein particles in adults receiving infliximab for chronic inflammatory disease, *JBMR Plus*, **5**, e10497, <https://doi.org/10.1002/jbm4.10497>.
28. Kunishige, R., Mizoguchi, M., Tsubouchi, A., Hanaoka, K., Miura, Y., Kurosu, H., Urano, Y., Kuro-O, M., and Murata, M. (2020) Calciprotein particle-induced cytotoxicity via lysosomal dysfunction and altered cholesterol distribution in renal epithelial HK-2 cells, *Sci. Rep.*, **10**, 20125, <https://doi.org/10.1038/s41598-020-77308-3>.
29. Kobylecki, C. J., Nordestgaard, B. G., and Afzal, S. (2021) Plasma ionized calcium and risk of cardio-

- vascular disease: 106,774 individuals from the Copenhagen General Population Study, *Clin. Chem.*, **67**, 265-275, <https://doi.org/10.1093/clinchem/hvaa245>.
30. Kobylecki, C. J., Nordestgaard, B. G., and Afzal, S. (2022) Low plasma ionized calcium is associated with increased mortality: a population-based study of 106,768 individuals, *J. Clin. Endocrinol. Metab.*, **107**, e3039-e3047, <https://doi.org/10.1210/clinem/dgac146>.
  31. Gimbrone, M. A., Jr., and García-Cardena, G. (2016) Endothelial cell dysfunction and the pathobiology of atherosclerosis, *Circ. Res.*, **118**, 620-636, <https://doi.org/10.1161/CIRCRESAHA.115.306301>.
  32. Mundi, S., Massaro, M., Scoditti, E., Carluccio, M. A., van Hinsbergh, V. W. M., Iruela-Arispe, M. L., and De Caterina, R. (2018) Endothelial permeability, LDL deposition, and cardiovascular risk factors – a review, *Cardiovasc. Res.*, **114**, 35-52, <https://doi.org/10.1093/cvr/cvx226>.
  33. Libby, P., Buring, J. E., Badimon, L., Hansson, G. K., Deanfield, J., Bittencourt, M. S., Tokgözoğlu, L., and Lewis, E. F. (2019) Atherosclerosis, *Nat. Rev. Dis. Primers*, **5**, 56, <https://doi.org/10.1038/s41572-019-0106-z>.
  34. Tamargo, I. A., Baek, K. I., Kim, Y., Park, C., and Jo, H. (2023) Flow-induced reprogramming of endothelial cells in atherosclerosis, *Nat. Rev. Cardiol.*, **20**, 738-753, <https://doi.org/10.1038/s41569-023-00883-1>.
  35. Wang, X., Shen, Y., Shang, M., Liu, X., and Munn, L. L. (2023) Endothelial mechanobiology in atherosclerosis, *Cardiovasc. Res.*, **119**, 1656-1675, <https://doi.org/10.1093/cvr/cvad076>.
  36. Giorgi, C., Marchi, S., and Pinton, P. (2018) The machineries, regulation and cellular functions of mitochondrial calcium, *Nat. Rev. Mol. Cell Biol.*, **19**, 713-730, <https://doi.org/10.1038/s41580-018-0052-8>.
  37. Walkon, L. L., Strubbe-Rivera, J. O., and Bazil, J. N. (2022) Calcium overload and mitochondrial metabolism, *Biomolecules*, **12**, 1891, <https://doi.org/10.3390/biom12121891>.
  38. De Nicolo, B., Cataldi-Stagetti, E., Diquigiovanni, C., and Bonora, E. (2023) Calcium and reactive oxygen species signaling interplays in cardiac physiology and pathologies, *Antioxidants (Basel)*, **12**, 353, <https://doi.org/10.3390/antiox12020353>.
  39. Werner, L. E., and Wagner, U. (2023) Calcium-sensing receptor-mediated NLRP3 inflammasome activation in rheumatoid arthritis and autoinflammation, *Front. Physiol.*, **13**, 1078569, <https://doi.org/10.3389/fphys.2022.1078569>.
  40. Mukai, H., Miura, Y., Kotani, K., Kotoda, A., Kurosu, H., Yamada, T., Kuro-O, M., and Iwazu, Y. (2022) The effects for inflammatory responses by CPP with different colloidal properties in hemodialysis patients, *Sci. Rep.*, **12**, 21856, <https://doi.org/10.1038/s41598-022-26166-2>.
  41. Bojic, M., Cejka, D., Bielez, B., and Schernthaner, G. H. (2023) Secondary calciprotein particle size is associated with patient mortality in peripheral artery disease, *Atherosclerosis*, **370**, 12-17, <https://doi.org/10.1016/j.atherosclerosis.2023.02.006>.
  42. Chen, W., Anokhina, V., Dieudonne, G., Abramowitz, M. K., Kashyap, R., Yan, C., Wu, T. T., de Mesy Bentley, K. L., Miller, B. L., and Bushinsky, D. A. (2019) Patients with advanced chronic kidney disease and vascular calcification have a large hydrodynamic radius of secondary calciprotein particles, *Nephrol. Dial. Transplant.*, **34**, 992-1000, <https://doi.org/10.1093/ndt/gfy117>.
  43. Chen, W., Fitzpatrick, J., Monroy-Trujillo, J. M., Sozio, S. M., Jaar, B. G., Estrella, M. M., Serrano, J., Anokhina, V., Miller, B. L., Melamed, M. L., Bushinsky, D. A., and Parekh, R. S. (2021) Associations of serum calciprotein particle size and transformation time with arterial calcification, arterial stiffness, and mortality in incident hemodialysis patients, *Am. J. Kidney Dis.*, **77**, 346-354, <https://doi.org/10.1053/j.ajkd.2020.05.031>.
  44. Feenstra, L., Reijrink, M., Pasch, A., Smith, E. R., Visser, L. M., Bulthuis, M., Lodewijk, M. E., Mastik, M. F., Greuter, M. J. W., Slart, R. H. J. A., Mulder, D. J., Pol, R. A., Te Velde-Keyzer, C. A., TransplantLines Investigators, Krenning, G., and Hillebrands, J. L. (2024) Calciprotein particle counts associate with vascular remodelling in chronic kidney disease, *Cardiovasc. Res.*, **120**, 1953-1966, <https://doi.org/10.1093/cvr/cvae164>.
  45. Zeper, L. W., Smith, E. R., Ter Braake, A. D., Tinnemans, P. T., de Baaij, J. H. F., and Hoenderop, J. G. J. (2023) Calciprotein particle synthesis strategy determines in vitro calcification potential, *Calcif. Tissue Int.*, **112**, 103-117, <https://doi.org/10.1007/s00223-022-01036-1>.
  46. Mencke, R., Al Ali, L., de Koning, M. L. Y., Pasch, A., Minnion, M., Feelisch, M., van Veldhuisen, D. J., van der Horst, I. C. C., Gansevoort, R. T., Bakker, S. J. L., de Borst, M. H., van Goor, H., van der Harst, P., Lipsic, E., and Hillebrands, J. L. (2024) Serum calcification propensity is increased in myocardial infarction and hints at a pathophysiological role independent of classical cardiovascular risk factors, *Arterioscler. Thromb. Vasc. Biol.*, **44**, 1884-1894, <https://doi.org/10.1161/ATVBAHA.124.320974>.
  47. Mori, K., Shoji, T., Nakatani, S., Uedono, H., Ochi, A., Yoshida, H., Imanishi, Y., Morioka, T., Tsujimoto, Y., Kuro-O, M., and Emoto, M. (2024) Differential associations of fetuin-A and calcification propensity with cardiovascular events and subsequent mortality in patients undergoing hemodialysis, *Clin. Kidney J.*, **17**, sfae042, <https://doi.org/10.1093/ckj/sfae042>.
  48. Van der Vaart, A., Eelderink, C., van Goor, H., Hillebrands, J. L., Te Velde-Keyzer, C. A., Bakker, S. J. L., Pasch, A., van Dijk, P. R., Laverman, G. D., and de Borst, M. H. (2024) Serum T50 predicts cardiovascular mortality in individuals with type 2 diabetes: a prospective cohort study, *J. Intern. Med.*, **295**, 748-758, <https://doi.org/10.1111/joim.13781>.

49. Miura, M., Miura, Y., Iwazu, Y., Mukai, H., Sugiura, T., Suzuki, Y., Kato, M., Kano, M., Nagata, D., Shiizaki, K., Kurosu, H., and Kuro-O, M. (2023) Removal of calciprotein particles from the blood using an adsorption column improves prognosis of hemodialysis miniature pigs, *Sci. Rep.*, **13**, 15026, <https://doi.org/10.1038/s41598-023-42273-0>.
50. Kawakami, K., Ohya, M., Yashiro, M., Sonou, T., Yamamoto, S., Nakashima, Y., Yano, T., Tanaka, Y., Ishida, K., Kobashi, S., Shigematsu, T., and Araki, S. I. (2023) Bisphosphonate FYB-931 prevents high phosphate-induced vascular calcification in rat aortic rings by altering the dynamics of the transformation of calciprotein particles, *Calcif. Tissue Int.*, **113**, 216-228, <https://doi.org/10.1007/s00223-023-01086-z>.
51. Rossi, A., Pizzo, P., and Filadi, R. (2019) Calcium, mitochondria and cell metabolism: a functional triangle in bioenergetics, *Biochim. Biophys. Acta Mol. Cell Res.*, **1866**, 1068-1078, <https://doi.org/10.1016/j.bbamcr.2018.10.016>.
52. Park, C. J., and Shin, R. (2022) Calcium channels and transporters: roles in response to biotic and abiotic stresses, *Front. Plant Sci.*, **13**, 964059, <https://doi.org/10.3389/fpls.2022.964059>.
53. Harlacher, E., Wollenhaupt, J., Baaten, C. C. F. M. J., and Noels, H. (2022) Impact of uremic toxins on endothelial dysfunction in chronic kidney disease: a systematic review, *Int. J. Mol. Sci.*, **23**, 531, <https://doi.org/10.3390/ijms23010531>.
54. Roumeliotis, S., Mallamaci, F., and Zoccali, C. (2020) Endothelial dysfunction in chronic kidney disease, from biology to clinical outcomes: a 2020 update, *J. Clin. Med.*, **9**, 2359, <https://doi.org/10.3390/jcm9082359>.
55. Kutikhin, A. G., Shishkova, D. K., Velikanova, E. A., Sinitsky, M. Y., Sinitskaya, A. V., and Markova, V. E. (2022) Endothelial dysfunction in the context of blood-brain barrier modeling, *J. Evol. Biochem. Physiol.*, **58**, 781-806, <https://doi.org/10.1134/S0022093022030139>.
56. Ferrucci, L., and Fabbri, E. (2018) Inflammageing: chronic inflammation in ageing, cardiovascular disease, and frailty, *Nat. Rev. Cardiol.*, **15**, 505-522, <https://doi.org/10.1038/s41569-018-0064-2>.
57. Liberale, L., Montecucco, F., Tardif, J. C., Libby, P., and Camici, G. G. (2020) Inflamm-ageing: the role of inflammation in age-dependent cardiovascular disease, *Eur. Heart J.*, **41**, 2974-2982, <https://doi.org/10.1093/eurheartj/ehz961>.
58. Walker, K. A., Basisty, N., Wilson, D. M., 3rd, and Ferrucci, L. (2022) Connecting aging biology and inflammation in the omics era, *J. Clin. Invest.*, **132**, e158448, <https://doi.org/10.1172/JCI158448>.
59. Li, X., Li, C., Zhang, W., Wang, Y., Qian, P., and Huang, H. (2023) Inflammation and aging: signaling pathways and intervention therapies, *Signal Transduct. Target Ther.*, **8**, 239, <https://doi.org/10.1038/s41392-023-01502-8>.
60. Kuro-O, M. (2021) Phosphate as a pathogen of arteriosclerosis and aging, *J. Atheroscler. Thromb.*, **28**, 203-213, <https://doi.org/10.5551/jat.RV17045>.
61. Tiong, M. K., Holt, S. G., Ford, M. L., and Smith, E. R. (2022) Serum calciprotein monomers and chronic kidney disease progression, *Am. J. Nephrol.*, **53**, 806-815, <https://doi.org/10.1159/000526609>.
62. Kuro-O, M. (2021) Klotho and calciprotein particles as therapeutic targets against accelerated ageing, *Clin. Sci. (Lond.)*, **135**, 1915-1927, <https://doi.org/10.1042/CS20201453>.
63. Gelli, R., Ridi, F., and Baglioni, P. (2019) The importance of being amorphous: calcium and magnesium phosphates in the human body, *Adv. Colloid Interface Sci.*, **269**, 219-235, <https://doi.org/10.1016/j.cis.2019.04.011>.
64. Pasch, A., Jahnlen-Dechent, W., and Smith, E. R. (2018) Phosphate, calcification in blood, and mineral stress: the physiologic blood mineral buffering system and its association with cardiovascular risk, *Int. J. Nephrol.*, **2018**, 9182078, <https://doi.org/10.1155/2018/9182078>.
65. Di Marco, G. S., Hausberg, M., Hillebrand, U., Rustemeyer, P., Wittkowski, W., Lang, D., and Pavenstädt, H. (2008) Increased inorganic phosphate induces human endothelial cell apoptosis *in vitro*, *Am. J. Physiol. Renal Physiol.*, **294**, F1381-F1387, <https://doi.org/10.1152/ajprenal.00003.2008>.
66. Shuto, E., Taketani, Y., Tanaka, R., Harada, N., Isshiki, M., Sato, M., Nashiki, K., Amo, K., Yamamoto, H., Higashi, Y., Nakaya, Y., and Takeda, E. (2009) Dietary phosphorus acutely impairs endothelial function, *J. Am. Soc. Nephrol.*, **20**, 1504-1512, <https://doi.org/10.1681/ASN.2008101106>.
67. Peng, A., Wu, T., Zeng, C., Rakheja, D., Zhu, J., Ye, T., Hutcheson, J., Vaziri, N. D., Liu, Z., Mohan, C., and Zhou, X. J. (2011) Adverse effects of simulated hyper- and hypo-phosphatemia on endothelial cell function and viability, *PLoS One*, **6**, e23268, <https://doi.org/10.1371/journal.pone.0023268>.
68. Yamada, S., Tokumoto, M., Tatsumoto, N., Taniguchi, M., Noguchi, H., Nakano, T., Masutani, K., Ooboshi, H., Tsuruya, K., and Kitazono, T. (2014) Phosphate overload directly induces systemic inflammation and malnutrition as well as vascular calcification in uremia, *Am. J. Physiol. Renal Physiol.*, **306**, F1418-F1428, <https://doi.org/10.1152/ajprenal.00633.2013>.
69. Voelkl, J., Egli-Spichtig, D., Alesutan, I., and Wagner, C. A. (2021) Inflammation: a putative link between phosphate metabolism and cardiovascular disease, *Clin. Sci. (Lond.)*, **135**, 201-227, <https://doi.org/10.1042/CS20190895>.
70. Ding, M., Zhang, Q., Zhang, M., Jiang, X., Wang, M., Ni, L., Gong, W., Huang, B., and Chen, J. (2022) Phosphate overload stimulates inflammatory reaction via PiT-1 and induces vascular calcification in uremia, *J. Ren. Nutr.*, **32**, 178-188, <https://doi.org/10.1053/j.jrn.2021.03.008>.

71. Hetz, R., Beeler, E., Janoczkin, A., Kiers, S., Li, L., Willard, B. B., Razzaque, M. S., and He, P. (2022) Excessive inorganic phosphate burden perturbed intracellular signaling: quantitative proteomics and phosphoproteomics analyses, *Front. Nutr.*, **8**, 765391, <https://doi.org/10.3389/fnut.2021.765391>.
72. Heiss, A., Eckert, T., Aretz, A., Richtering, W., van Dorp, W., Schäfer, C., and Jahnen-Dechent, W. (2008) Hierarchical role of fetuin-A and acidic serum proteins in the formation and stabilization of calcium phosphate particles, *J. Biol. Chem.*, **283**, 14815-14825, <https://doi.org/10.1074/jbc.M709938200>.
73. Dridi, H., Kushnir, A., Zalk, R., Yuan, Q., Melville, Z., and Marks, A. R. (2020) Intracellular calcium leak in heart failure and atrial fibrillation: a unifying mechanism and therapeutic target, *Nat. Rev. Cardiol.*, **17**, 732-747, <https://doi.org/10.1038/s41569-020-0394-8>.
74. Arnold, A., Dennison, E., Kovacs, C. S., Mannstadt, M., Rizzoli, R., Brandi, M. L., Clarke, B., and Thakker, R. V. (2021) Hormonal regulation of biomineralization, *Nat. Rev. Endocrinol.*, **17**, 261-275, <https://doi.org/10.1038/s41574-021-00477-2>.
75. Collins, M. T., Marcucci, G., Anders, H. J., Beltrami, G., Cauley, J. A., Ebeling, P. R., Kumar, R., Linglart, A., Sangiorgi, L., Towler, D. A., Weston, R., Whyte, M. P., Brandi, M. L., Clarke, B., and Thakker, R. V. (2022) Skeletal and extraskeletal disorders of biomineralization, *Nat. Rev. Endocrinol.*, **18**, 473-489, <https://doi.org/10.1038/s41574-022-00682-7>.
76. Shishkova, D. K., Sinitskaya, A. V., Sinitsky, M. Y., Matveeva, V. G., Velikanova, E. A., Markova, V. E., and Kutikhin, A. G. (2022) Spontaneous endothelial-to-mesenchymal transition in human primary umbilical vein endothelial cells, *Compl. Iss. Cardiovasc. Dis.*, **11**, 97-114, <https://doi.org/10.17802/2306-1278-2022-11-3-97-114>.
77. Bogdanov, L. A., Velikanova, E. A., Kanonykina, A. Y., Frolov, A. V., Shishkova, D. K., Lazebnaya, A. I., and Kutikhin, A. G. (2022) Vascular smooth muscle cell contractile proteins as universal markers of vessels of microcirculatory bed, *Compl. Iss. Cardiovasc. Dis.*, **11**, 162-176, <https://doi.org/10.17802/2306-1278-2022-11-3-162-176>.
78. Wang, B., Han, J., Elisseeff, J. H., and Demaria, M. (2024) The senescence-associated secretory phenotype and its physiological and pathological implications, *Nat. Rev. Mol. Cell Biol.*, **25**, 958-978, <https://doi.org/10.1038/s41580-024-00727-x>.
79. Mehdizadeh, M., Aguilar, M., Thorin, E., Ferbeyre, G., and Nattel, S. (2022) The role of cellular senescence in cardiac disease: basic biology and clinical relevance, *Nat. Rev. Cardiol.*, **19**, 250-264, <https://doi.org/10.1038/s41569-021-00624-2>.
80. Di Micco, R., Krizhanovsky, V., Baker, D., and d'Adda di Fagagna, F. (2021) Cellular senescence in ageing: from mechanisms to therapeutic opportunities, *Nat. Rev. Mol. Cell Biol.*, **22**, 75-95, <https://doi.org/10.1038/s41580-020-00314-w>.
81. Ewence, A. E., Bootman, M., Roderick, H. L., Skepper, J. N., McCarthy, G., Eppe, M., Neumann, M., Shanahan, C. M., and Proudfoot, D. (2008) Calcium phosphate crystals induce cell death in human vascular smooth muscle cells: a potential mechanism in atherosclerotic plaque destabilization, *Circ. Res.*, **103**, e28-e34, <https://doi.org/10.1161/CIRCRESAHA.108.181305>.
82. Jäger, E., Murthy, S., Schmidt, C., Hahn, M., Strobel, S., Peters, A., Stäubert, C., Sungur, P., Venus, T., Geisler, M., Radusheva, V., Raps, S., Rothe, K., Scholz, R., Jung, S., Wagner, S., Pierer, M., Seifert, O., Chang, W., Estrela-Lopis, I., Raulien, N., Krohn, K., Sträter, N., Hoepfener, S., Schöneberg, T., Rossol, M., and Wagner, U. (2020) Calcium-sensing receptor-mediated NLRP3 inflammasome response to calciprotein particles drives inflammation in rheumatoid arthritis, *Nat. Commun.*, **11**, 4243, <https://doi.org/10.1038/s41467-020-17749-6>.
83. Tournis, S., Makris, K., Cavalier, E., and Trovas, G. (2020) Cardiovascular risk in patients with primary hyperparathyroidism, *Curr. Pharm. Des.*, **26**, 5628-5636, <https://doi.org/10.2174/1381612824999201105165642>.
84. Bkaily, G., and Jacques, D. (2023) Calcium homeostasis, transporters, and blockers in health and diseases of the cardiovascular system, *Int. J. Mol. Sci.*, **24**, 8803, <https://doi.org/10.3390/ijms24108803>.
85. Minisola, S., Arnold, A., Belaya, Z., Brandi, M. L., Clarke, B. L., Hannan, F. M., Hofbauer, L. C., Insogna, K. L., Lacroix, A., Liberman, U., Palermo, A., Pepe, J., Rizzoli, R., Wermers, R., and Thakker, R. V. (2022) Epidemiology, pathophysiology, and genetics of primary hyperparathyroidism, *J. Bone Miner. Res.*, **37**, 2315-2329, <https://doi.org/10.1002/jbmr.4665>.
86. Tonon, C. R., Silva, T. A. A. L., Pereira, F. W. L., Queiroz, D. A. R., Junior, E. L. F., Martins, D., Azevedo, P. S., Okoshi, M. P., Zornoff, L. A. M., de Paiva, S. A. R., Minicucci, M. F., and Polegato, B. F. (2022) A review of current clinical concepts in the pathophysiology, etiology, diagnosis, and management of hypercalcemia, *Med. Sci. Monit.*, **28**, e935821, <https://doi.org/10.12659/MSM.935821>.
87. Lang, I. M., and Schleef, R. R. (1996) Calcium-dependent stabilization of type I plasminogen activator inhibitor within platelet alpha-granules, *J. Biol. Chem.*, **271**, 2754-2761, <https://doi.org/10.1074/jbc.271.5.2754>.
88. Liu, Q., Möller, U., Flügel, D., and Kietzmann, T. (2004) Induction of plasminogen activator inhibitor I gene expression by intracellular calcium via hypoxia-inducible factor-1, *Blood*, **104**, 3993-4001, <https://doi.org/10.1182/blood-2004-03-1017>.
89. Peiretti, F., Fossat, C., Anfosso, F., Alessi, M. C., Henry, M., Juhan-Vague, I., and Nalbone, G. (1996) Increase in cytosolic calcium upregulates the synthesis

- of type 1 plasminogen activator inhibitor in the human histiocytic cell line U937, *Blood*, **87**, 162-173, <https://doi.org/10.1182/blood.V87.1.162.162>.
90. Heiss, A., DuChesne, A., Denecke, B., Grötzinger, J., Yamamoto, K., Renné, T., and Jahnen-Dechent, W. (2003) Structural basis of calcification inhibition by alpha 2-HS glycoprotein/fetuin-A: formation of colloidal calciprotein particles, *J. Biol. Chem.*, **278**, 13333-13341, <https://doi.org/10.1074/jbc.M210868200>.
91. Schäfer, C., Heiss, A., Schwarz, A., Westenfeld, R., Ketteler, M., Floege, J., Müller-Esterl, W., Schinke, T., and Jahnen-Dechent, W. (2003) The serum protein alpha 2-Heremans-Schmid glycoprotein/fetuin-A is a systemically acting inhibitor of ectopic calcification, *J. Clin. Invest.*, **112**, 357-366, <https://doi.org/10.1172/JCI17202>.
92. Heiss, A., Jahnen-Dechent, W., Endo, H., and Schwahn, D. (2007) Structural dynamics of a colloidal protein-mineral complex bestowing on calcium phosphate a high solubility in biological fluids, *Biointerphases*, **2**, 16-20, <https://doi.org/10.1116/1.2714924>.
93. Rochette, C. N., Rosenfeldt, S., Heiss, A., Narayanan, T., Ballauff, M., and Jahnen-Dechent, W. (2009) A shielding topology stabilizes the early stage protein-mineral complexes of fetuin-A and calcium phosphate: a time-resolved small-angle X-ray study, *ChemBiochem*, **10**, 735-740, <https://doi.org/10.1002/cbic.200800719>.

**Publisher's Note.** Pleiades Publishing remains neutral with regard to jurisdictional claims in published maps and institutional affiliations. AI tools may have been used in the translation or editing of this article.